Two-Particle Bose–Einstein Correlations in *pp* Collisions at 13 TeV with ATLAS at LHC

<u>Yuri Kulchitsky</u>, E.Plotnikova, N. Russakovich, P. Tsiareshka

JINR, Dubna, Russia

B. I. Stepanov Institute of Physics NAS, Minsk, Belarus

XV-th International School-Conference "The Actual Problems of Microworld Physics"

27 August – 3 September 2023, Minsk, Belarus,

Motivation for Bose-Einstein correlations

- Bose-Einstein correlations (BEC) represent a unique probe of the *space-time geometry* of the *hadronization region* and allow the *determination the size and shape of the source* from which particles are *emitted*.

- Studies of the dependence of BEC on *particle multiplicity* and *transverse momentum* are of special interest. They help in the understanding of multiparticle production mechanisms.

- High-multiplicity data in proton interactions can serve as a reference for studies in nucleus-nucleus collisions. The effect is reproduced in hydrodynamical and Pomeron-based approaches for hadronic interactions where high multiplicities play a crucial role.

BOSE-EINSTEIN CORRELATIONS AND HANBURY BROWN –TWISS INTERFEROMETRY

Bose-Einstein correlations (BEC) are often considered to be the analogue of the Robert **Hanbury Brown** and Richard **Twiss** (**HBT**) effect in astronomy, describing the interference of incoherently-emitted identical bosons

Intensity interferometry of photons in radio-astronomy:

- **measures angular diameter of two stars, so the physical size of the source**

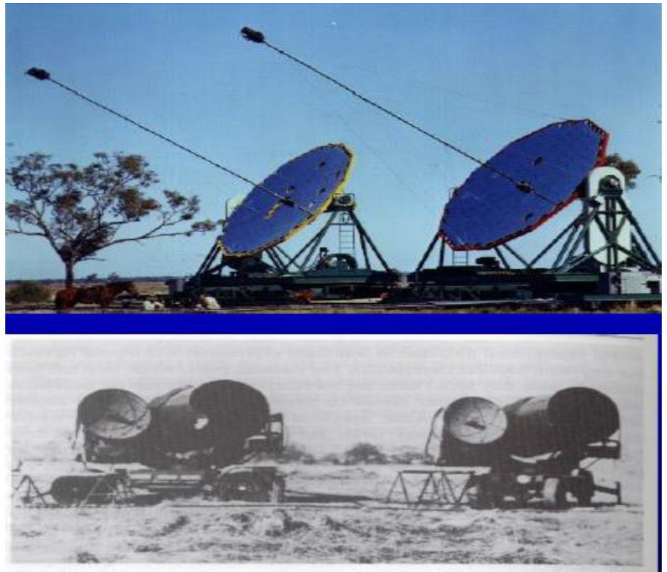

Figure 10.1 The first stellar intensity interferometer; the pilot model of the stellar intensity interferometer at Jodrell Bank in 1955. Two Army searchlights were used to make the first measurement of the angular diameter of a main sequence star (Sirius).

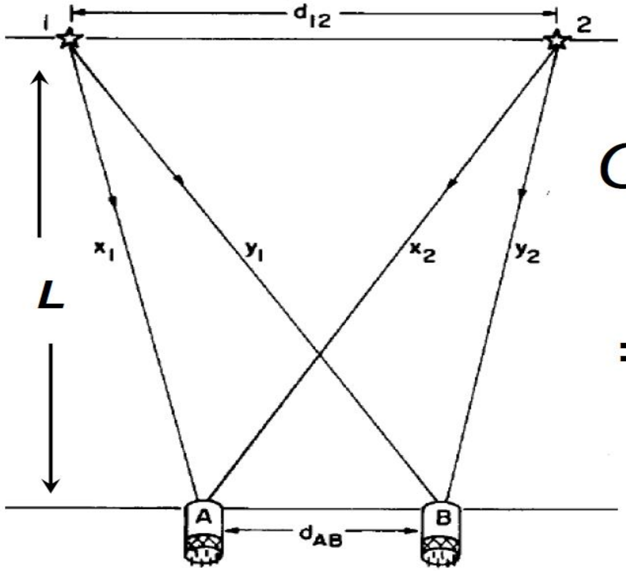

$$C(d) = \frac{\langle I_1 I_2 \rangle}{\langle I_1 \rangle \langle I_2 \rangle}$$

$$= 1 + A\cos(d_{AB})$$

$$d_{AB} = \lambda/\theta$$

$I_{1(2)}$ - intensities, $<x>$ - averaging over random phases

λ is the wavelength of the light, $\theta = d_{12}/L$

Varying $\boldsymbol{d_{AB}}$ one learns the angle, and using the individual wave vectors, the physical size of the source

Roy Jay ***Glauber*** - awarded in 2005 Nobel Prize in Physics

"for his contribution to the quantum theory of optical coherence"

Bose-Einstein Correlations

Correlations in phase space **between two identical bosons** from symmetry of wave functions.

► Enhances likelihood of *two particles close* in phase space

► Allows one to 'probe' the source of the bosons *in size* and *shape*

► Dependence on particle multiplicity and transverse momentum probes *the production mechanism*

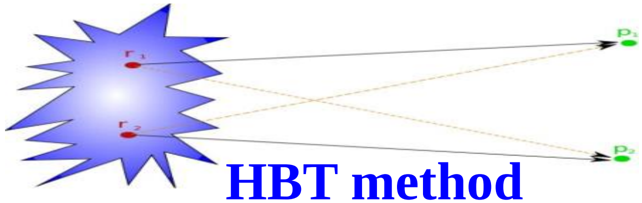

HBT method

Correlation function $C_2(Q)$ a ratio of probabilities:

$$C_2(Q) = \frac{\rho(p_1, p_2)}{\rho_0(p_1, p_2)} = C_0\left(1 + \Omega(\lambda, RQ)\right)\cdot\left(1 + Q\varepsilon\right),$$

$$\Omega^E(\lambda, RQ) = \lambda e^{-RQ}$$

$$\Omega^G(\lambda, RQ) = \lambda e^{-R^2Q^2}$$

$$Q^2 = -(p_1 - p_2)^2$$

$\mathbf{C_0}$ is a *normalisation*, **ε** accounts for *long range effects*, **R** is the **effective radius parameter of the source**, **λ** is the **strength of the effect parameter**, 0/1 for coherent/chaotic source.

Two possible parameterisation: **Gaussian and Exponential**.

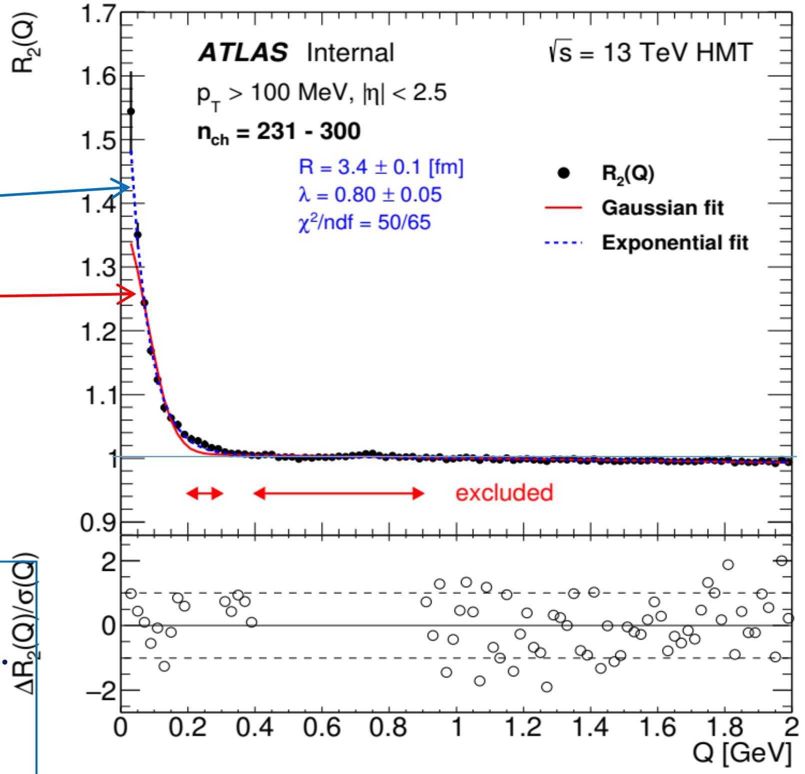

$$C_2(Q) = \frac{N^{++,--}(Q)}{N^{ref}(Q)}$$

$\mathbf{N_{ref}}$ **without BEC effect from:** unlike-charge particles (**UCP**), opposite hemispheres, event mixing. **Basic Reference**: distribution of **UCP** pairs of non-identical particle taken from the same event.

$$R_2(Q) = \frac{C_2^{Data}(Q)}{C_2^{MC}(Q)} = \frac{\rho(++,--)\big/\rho(+-)}{\rho^{MC}(++,--)\big/\rho^{MC}(+-)}$$

The studies are carried out using the **double ratio correlation function**. The $\mathbf{R_2(Q)}$ eliminates problems with energy-momentum conservation, topology, resonances, hadronic jets, mini-jets etc. **MC without BEC.**

A TOROIDAL LHC APPARATUS (ATLAS)

Subdetector	Operational Fraction
AFP	93.8%
ALFA	99.9%
CSC Cathode Strip Chambers	95.3%
Forward LAr Calorimeter	99.7%
Hadronic End-Cap Lar Cal	99.5%
LAr EM Calorimeter	100 %
LVL1 Calo Trigger	99.9%
LVL1 Muon RPC Trigger	99.8%
LVL1 Muon TGC Trigger	99.9%
MDT Muon Drift Tubes	99.7%
Pixels	97.8%
RPC Barrel Muon Chambers	94.4%
SCT Silicon Strips	98.7%
TGC End-Cap Muon Cha	99.5%
Tile Calorimeter	99.2%
TRT Transit Rad Tracker	97.2%

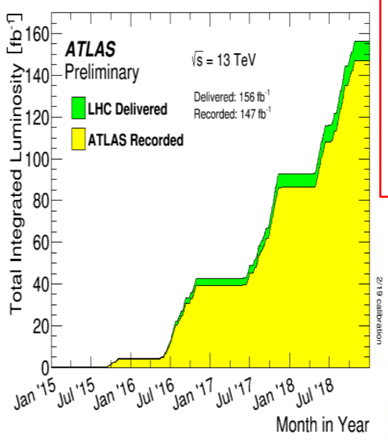

Air-core Muon spectrometer
(*μ Trigger/tracking and* ***Toroid Magnets***)
Precision Tracking:
MDT (Monitored Drift Tubes)
CSC (Cathode Strip Chambers) |η| >2.4
Trigger:
RPC (Resistive Plate Chamber) barrel
TGC (Thin Gas Chamber) endcap

Longitudinally segmented Calorimeter:
EM and Hadronic energy
LiquidAr EM barrel and End-cap & Hadronic End-cap
Tile calorimeter (Fe-scintillator) Hadronic barrel

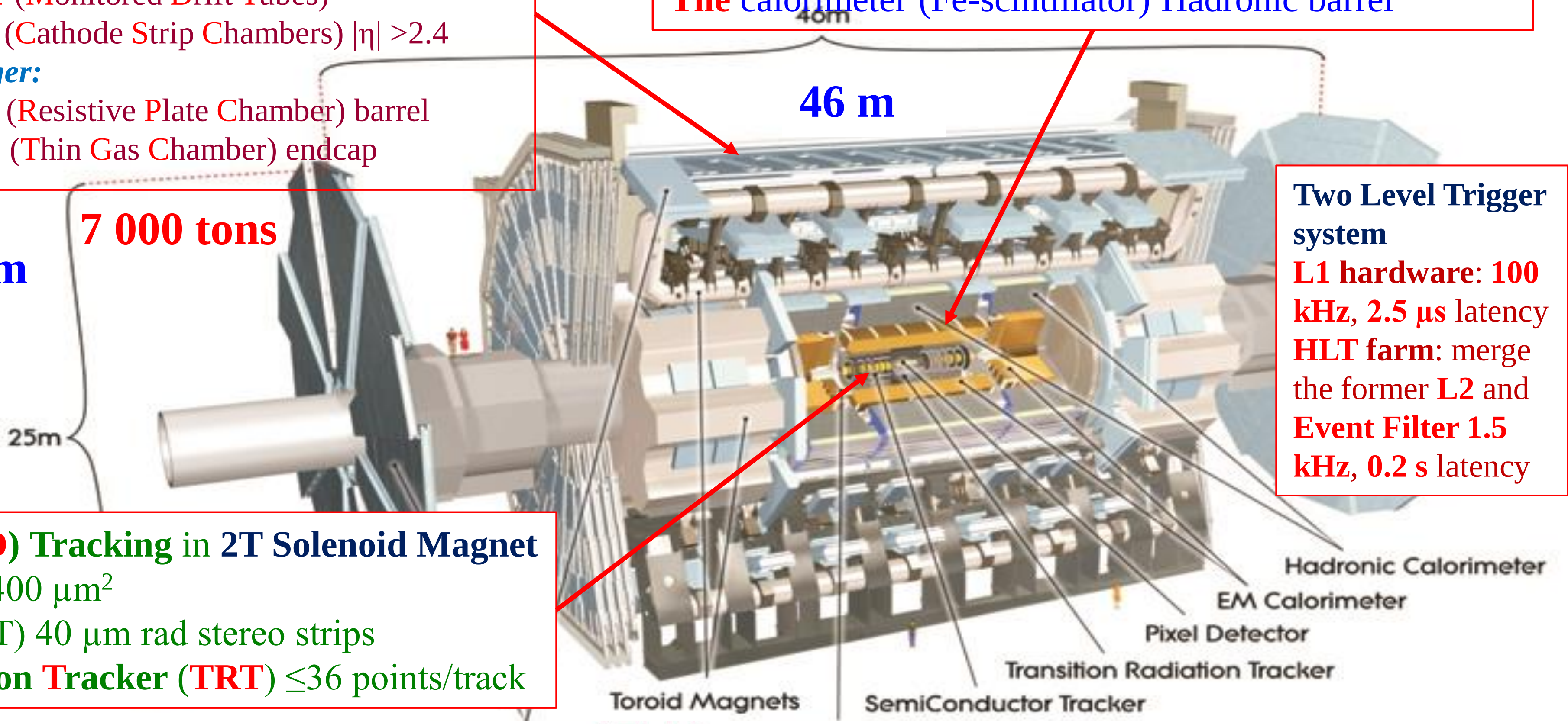

Two Level Trigger system
L1 hardware: **100 kHz, 2.5 μs** latency
HLT farm: merge the former **L2** and **Event Filter 1.5 kHz, 0.2 s** latency

Inner Detector (ID) Tracking in **2T Solenoid Magnet**
Silicon Pixels 50x400 μm^2
Silicon Strips (SCT) 40 μm rad stereo strips
TransitionRadiation Tracker (TRT) ≤36 points/track

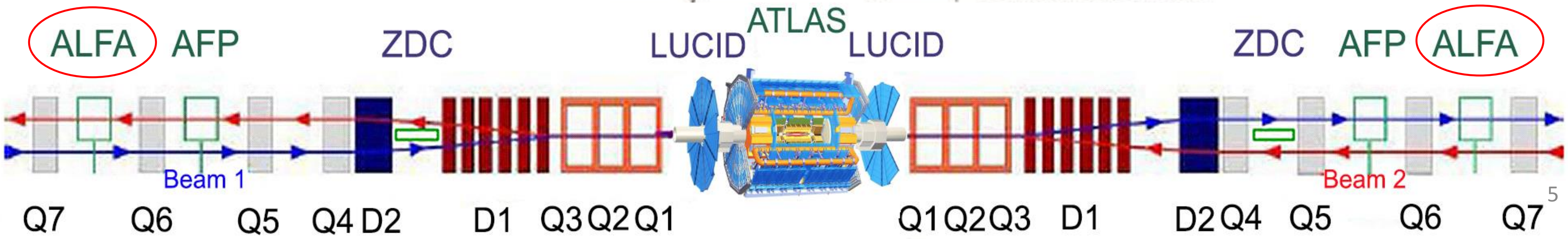

INNER DETECTORS (ID)

The focus of ATLAS is high-p_T physics and provides a window onto important *softer QCD processes.*
These have intrinsic interest but also the searches for new physics.

- ***Charged-particle distributions at √s=13 TeV in pp interactions***
- ***Charged-particle distributions sensitive to the underlying event in pp collisions at √s=13 TeV***

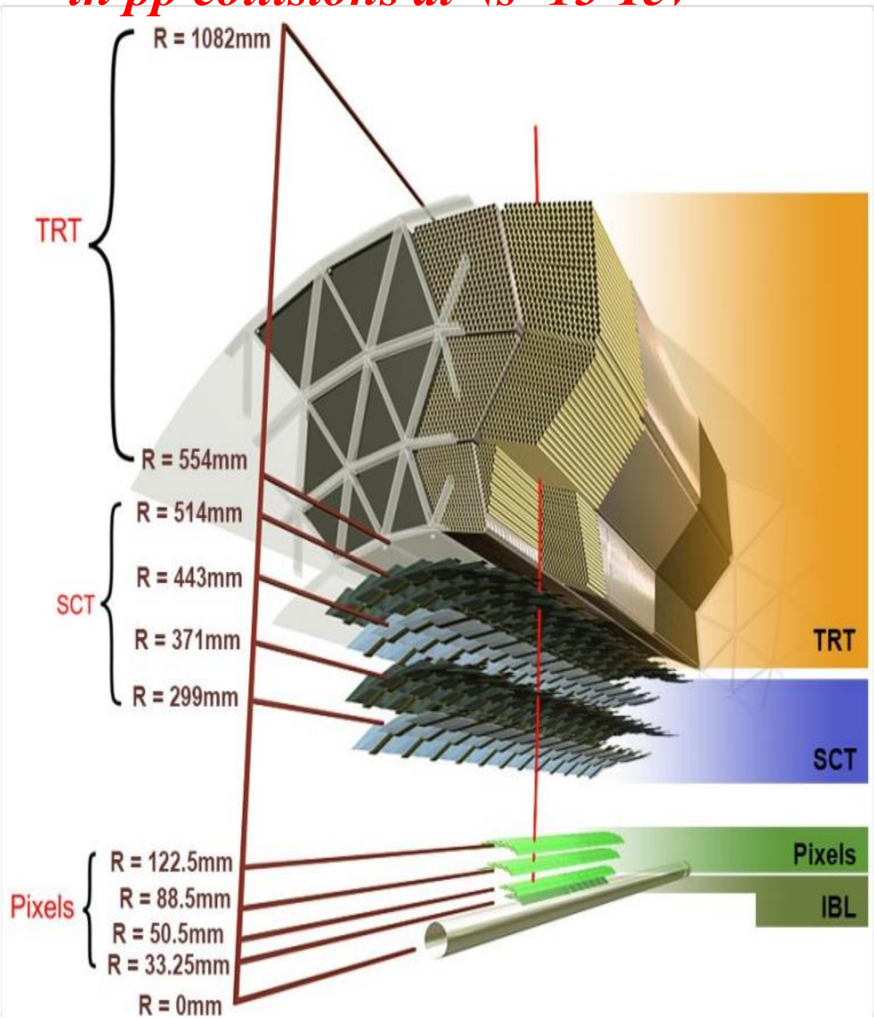

ATLAS tracking detectors:
Pixels, SCT & TRT

- **New innermost 4-th layer** for the Pixel detector [**IBL** = Insertable B-Layer]
- Required complete removal of the ATLAS Pixel volume
- IBL fully operational

New Be beam pipe

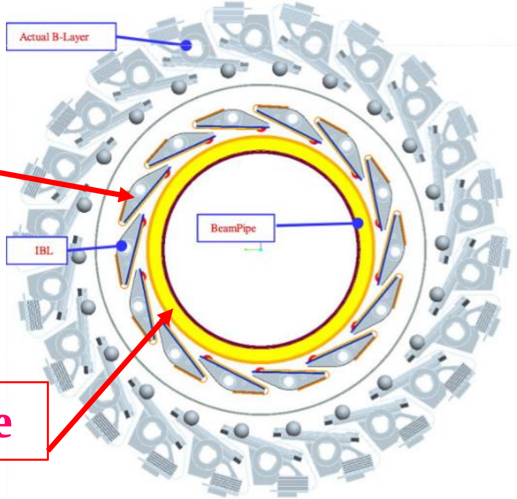

Two times better tracks impact parameters resolution at 13 TeV!

MINIMUM BIAS TRIGGER SCINTILLATOR

24 independent wedge-shaped plastic scintillators (12 per side) read out by PMTs,

2.08<|η|<3.86

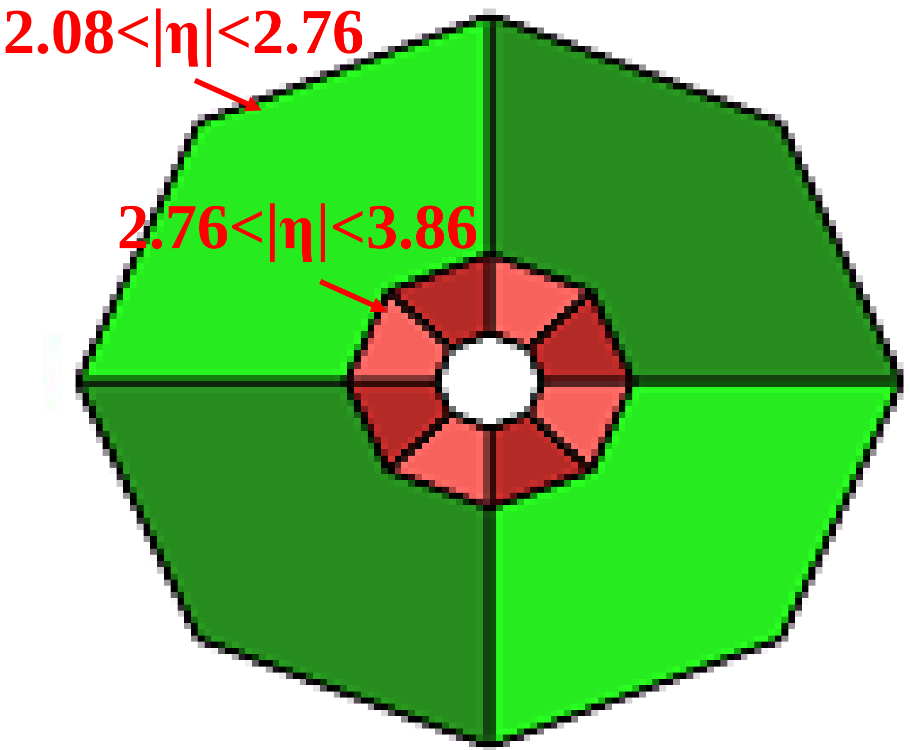

Pseudorapidity is defined as

$\eta = -\frac{1}{2}\ln(\tan(\theta/2))$

θ is the polar angle with respect to the beam.

- Designed for triggering on min bias events, >99% efficiency
- MBTS timing used to veto halo and beam gas events
- Also being used as gap trigger for various diffractive subjects

Minimum-Bias and High Multiplicity Track Triggers

ATLAS EXPERIMENT

- For these analysis the events collected with **Minimum-bias (MB)** trigger named as ***HLT_noalg_mb_L1MBTS _1*** are used.
  - This trigger required at least one hit in one of the 12+12 sectors (A and C sides) of the MBTS detector.

✓ ***Integral Luminosity ~151 μb^{-1}; Statistic: 9.6×10^{6} events with 2.4×10^{8} tracks***

- For these analysis the events collected with **High multiplicity track (HMT)** trigger named as ***HLT_mb_sp900_trk60_hmt_L1MBTS_1_1*** are used.
  - HMT events were collected at 13 TeV using a dedicated HMT trigger:
    - requires more than **900 SCT** space-points,
    - more than **60 reconstructed** good quality charged **tracks** with **p_T>0.4 GeV** associated with the primary vertex.

✓ ***Integral Luminosity ~8.4 nb^{-1}; Statistic: 9.1×10^{6} events with 9.8×10^{8} tracks***

Example of Very-High-Multiplicity event

High-multiplicity event with 319 reconstructed tracks.
The shown tracks are from a single vertex and have $p_T > 0.4$ GeV

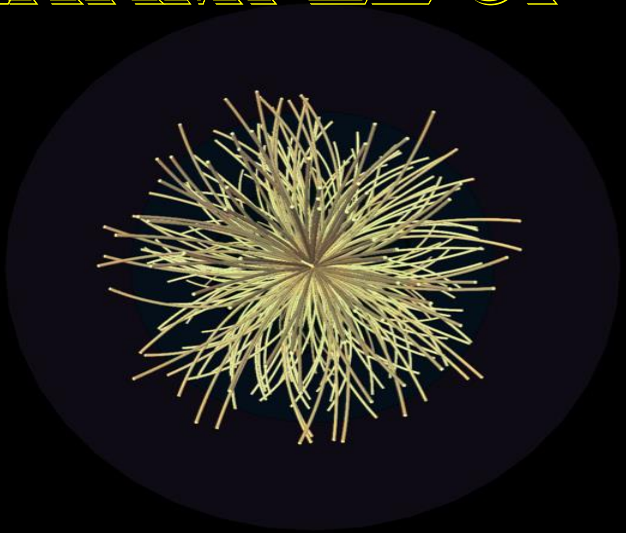

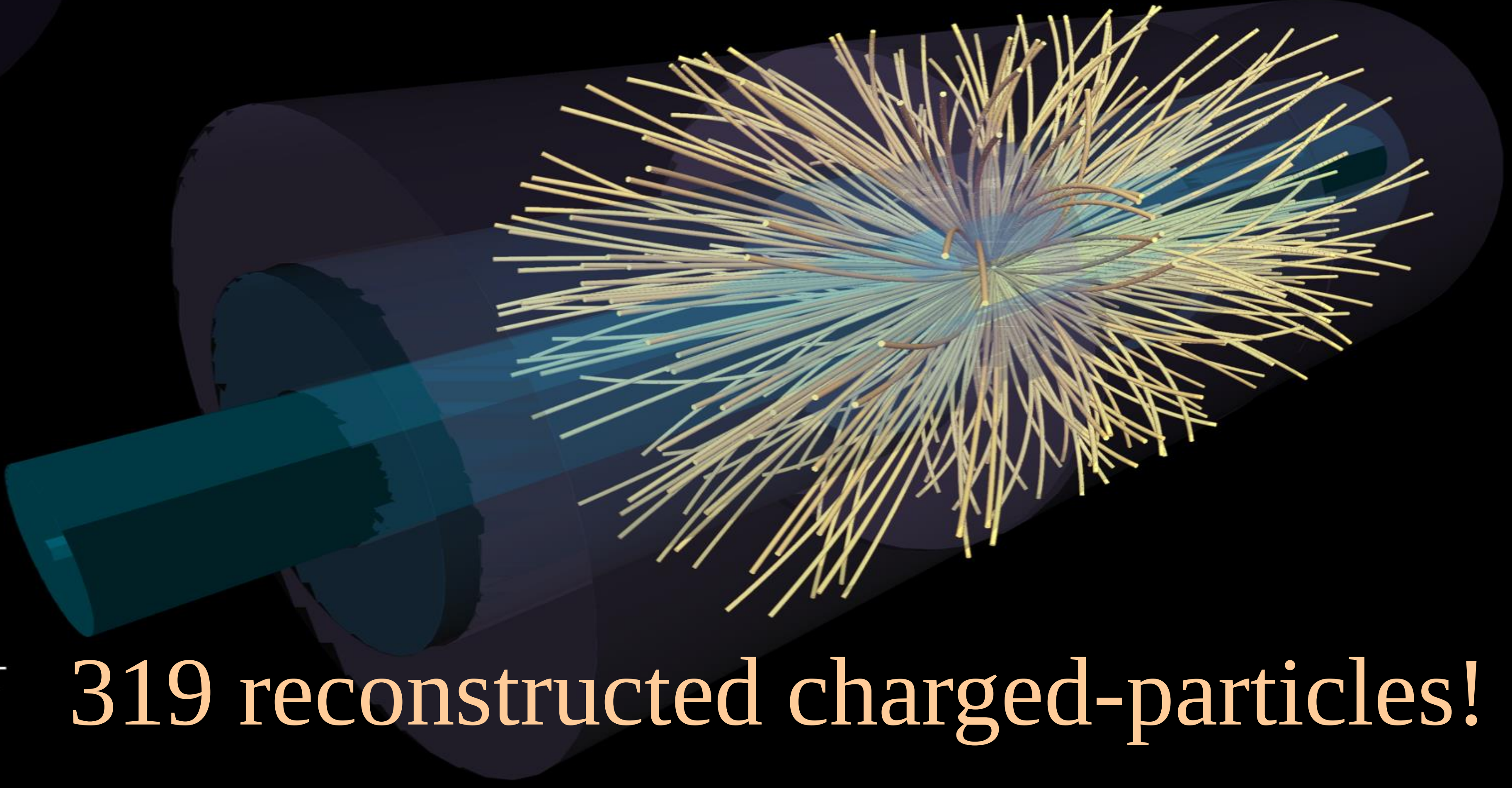

ATLAS EXPERIMENT

Run: 312837
Event: 135456971
2016-11-14 07:42:28 CEST

319 reconstructed charged-particles!

Example of Very-High-Multiplicity event

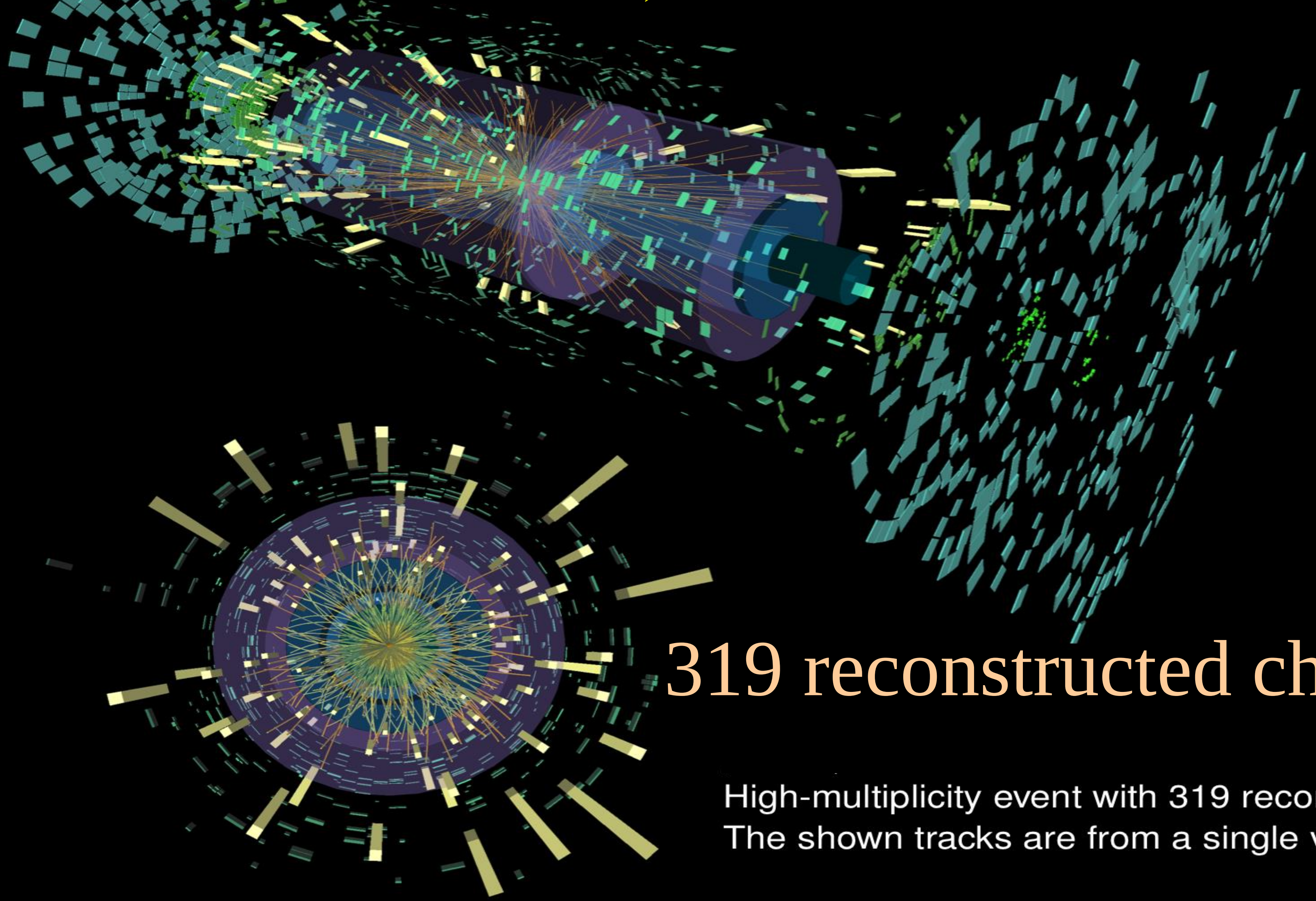

ATLAS EXPERIMENT

Run: 312837
Event: 135456971
2016-11-14 07:42:28 CEST

319 reconstructed charged-particles

High-multiplicity event with 319 reconstructed tracks.
The shown tracks are from a single vertex and have $p_T > 0.4$ GeV

CRUCIAL FEATURE FOR REFERENCE SAMPLE

1. Absence of Bose-Einstein correlations

2. Presence of correlations due to energy-momentum *and charge* ***conservation***

3. Presence of correlations due to the topology and the global properties ***of the events***

4. Absence of additional dynamical correlations due to Jets

5. Absence of additional dynamical correlations due to resonances of long-lived particle decays (η, ω, ρ, …)

- In the analysis used the reference sample: **UCP** pair combinations in an event
- UCP method ***satisfies*** **Conditions 1 – 3**, but not **Condition 5** (regions were excluded)
- $R_2(Q)$ correlation functions satisfy **Conditions 4 and 5**
- For OHP reference samples there are problems with **Conditions 2 – 4**

Comparison of two-particle correlation functions UCP/OHP

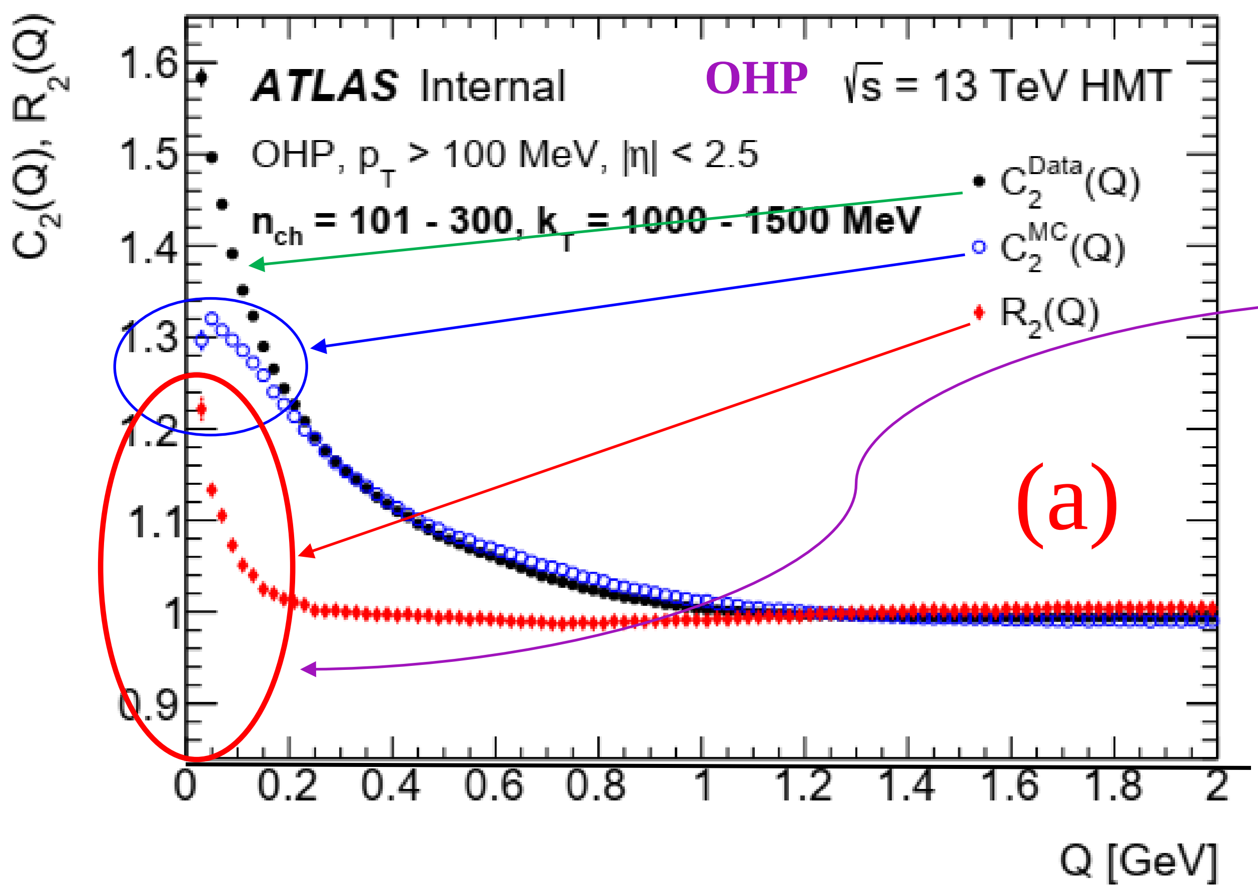

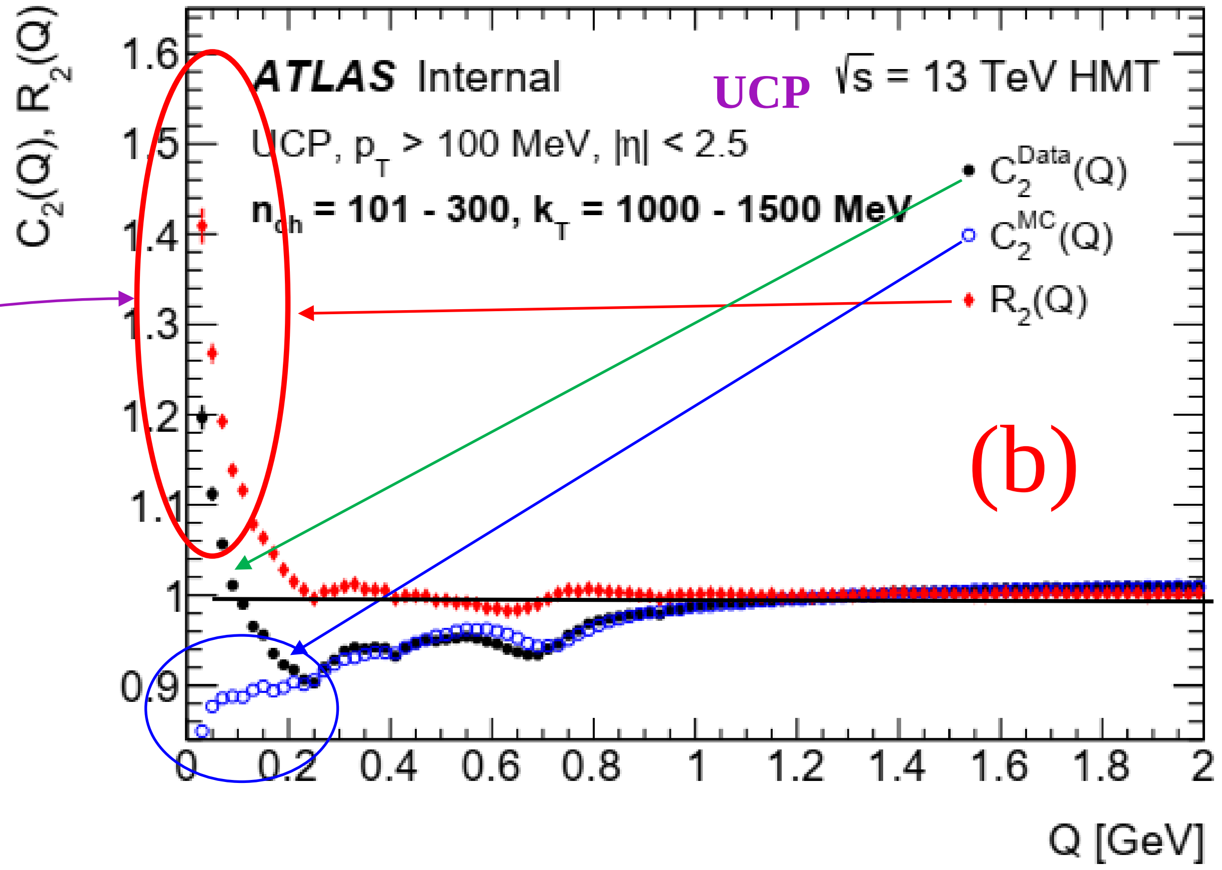

Comparison of single-ratio two-particle correlation functions, ***$C_2^{\text{data}}(Q)$* and *$C_2^{\text{MC}}(Q)$***, with two-particle double-ratio correlation function, ***$R_2(Q)$*,** for the HMT events using

(a) the **OHP** like-charge particles pairs reference sample for ***k_T*-interval 1.0 < *$k_T \leq$* 1.5 GeV;**

(b) the **UCP** pairs reference sample for ***k_T*-interval 1.0 < *$k_T \leq$* 1.5 GeV.**

SYSTEMATIC

Systematic uncertainties (in percent) in the correlation strength, λ, and source radius, R, for the exponential fit of the two-particle double-ratio correlation functions, $R_2(Q)$, for p_T>100 MeV at $\sqrt{s}$ = 13 TeV for the MB and HMT events

Sources of systematic uncertainty	Uncertainties for MB events [%]				Uncertainties for HMT events [%]			
	λ	R	λ	R	λ	R	λ	R
	Spread for n_{ch} distribution		For inclusive R_2 function		Spread for n_{ch} distribution		For inclusive R_2 function	
Track splitting and merging	negligible				negligible			
Track reconstr. efficiency	0.0–0.4	0.1–0.4	0.3	0.1	0.1–0.2	0.01–0.1	0.2	0.01
Unfolding matrix	0.0–0.3	0.0–0.1	0.01	0.0	0.0–0.4	0.0–0.1	0.01	0.03
MC generators (↑)	0.0–28.	0.0–21.	2.7	4.9	0.0–7.1	4.4–6.6	5.2	5.6
MC generators (↓)	0.0–12.	0.0–29.	5.4	5.8	1.4–9.9	0.0–11.	1.6	2.3
Coulomb correction	1.3–2.0	0.01–0.6	1.8	0.1	1.7–1.9	0.2–0.4	1.8	0.3
Fitted range of Q	0.0–0.5	0.02–0.9	0.2	0.3	0.0–0.2	0.0–0.2	0.02	0.03
Starting value of Q	0.0–1.9	0.01–1.1	0.3	0.2	0.5–1.4	0.3–0.7	0.7	0.4
Bin size	0.0–2.4	0.1–1.5	0.8	0.4	1.0–1.7	0.4–0.9	1.3	0.6
Exclusion intervals	0.0–1.1	0.3–0.8	0.1	0.3	0.4–0.6	0.3–0.6	0.5	0.5
Cumulative uncertainty (↑)	1.3–28.	1.2–21.	3.9	5.0	2.9–7.6	4.6–6.7	5.6	5.7
Cumulative uncertainty (↓)	2.4–12.	1.2–29.	5.9	5.8	2.8–10.	1.1–11.	2.6	2.5

SYSTEMATIC: COMPARISON OF MC BEC RESULTS

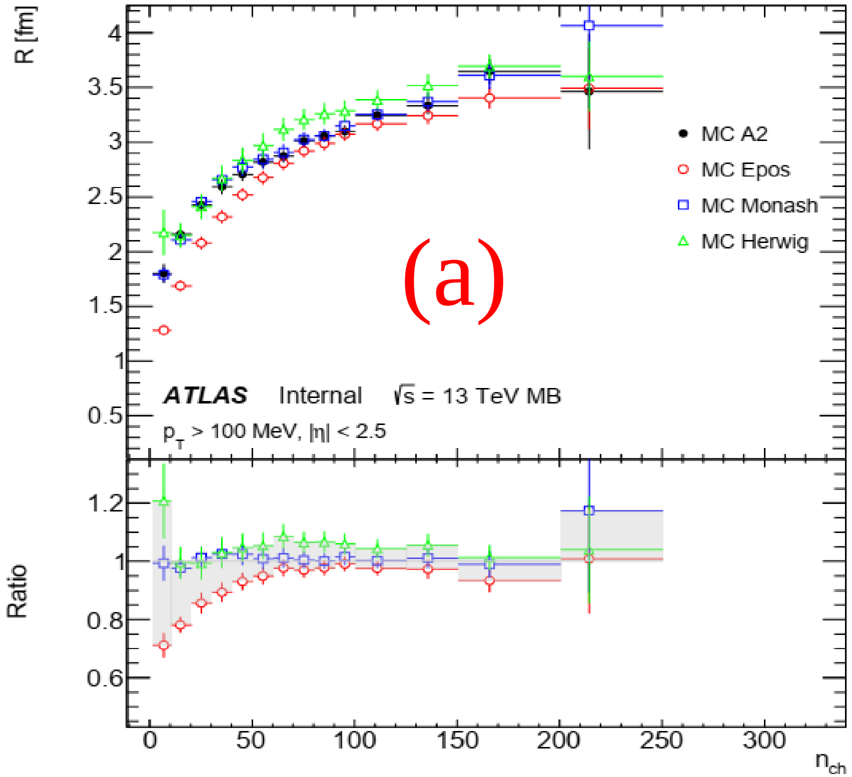

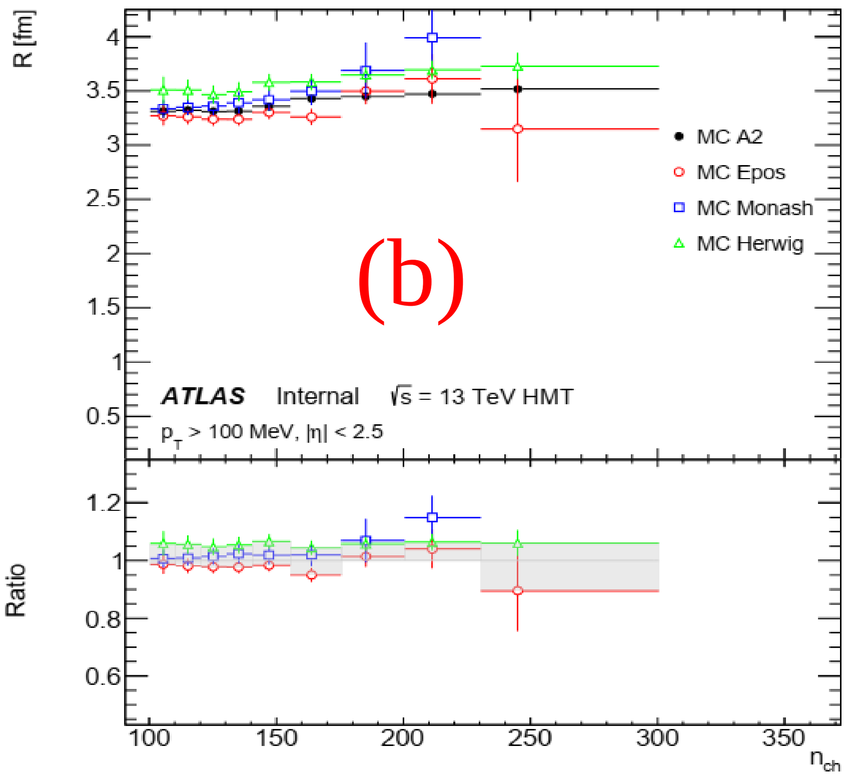

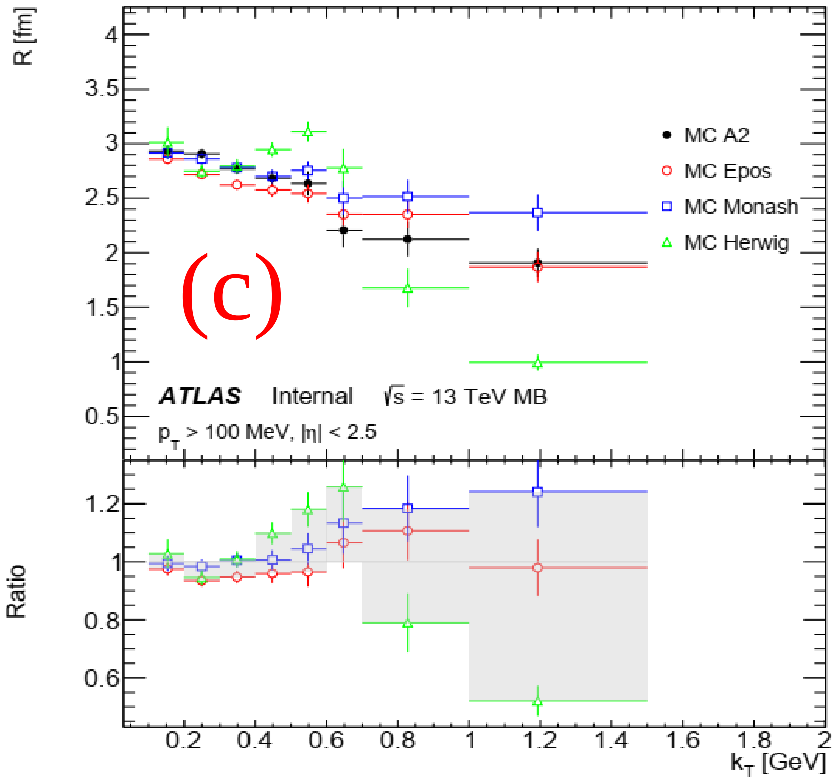

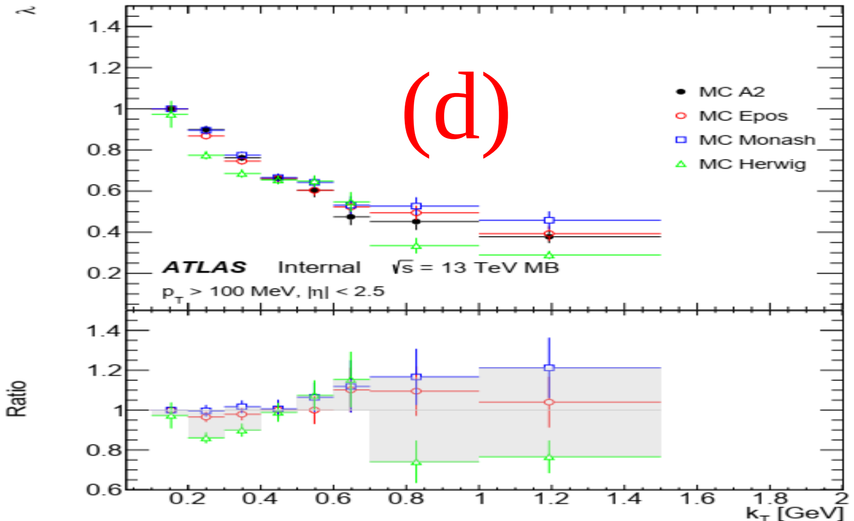

- The BEC parameters λ and R as a function of n_{ch} and k_T using different MC generators in the calculation of $R_2(Q)$. (a) R versus n_{ch} for MB events, (b) R versus n_{ch} for HMT events, (c) R versus k_T for MB events and (d) λ versus k_T for MB events. The uncertainties shown are statistical.
- The lower panel of each plot shows the ratio of the BEC parameters obtained using **EPOS LHC**, **Pythia 8 Monash** and **Herwig++ UE-EE-5** compared with the parameters obtained using **Pythia 8 A2**.

THE TWO-PARTICLE DOUBLE-RATIO CORRELATION FUNCTION

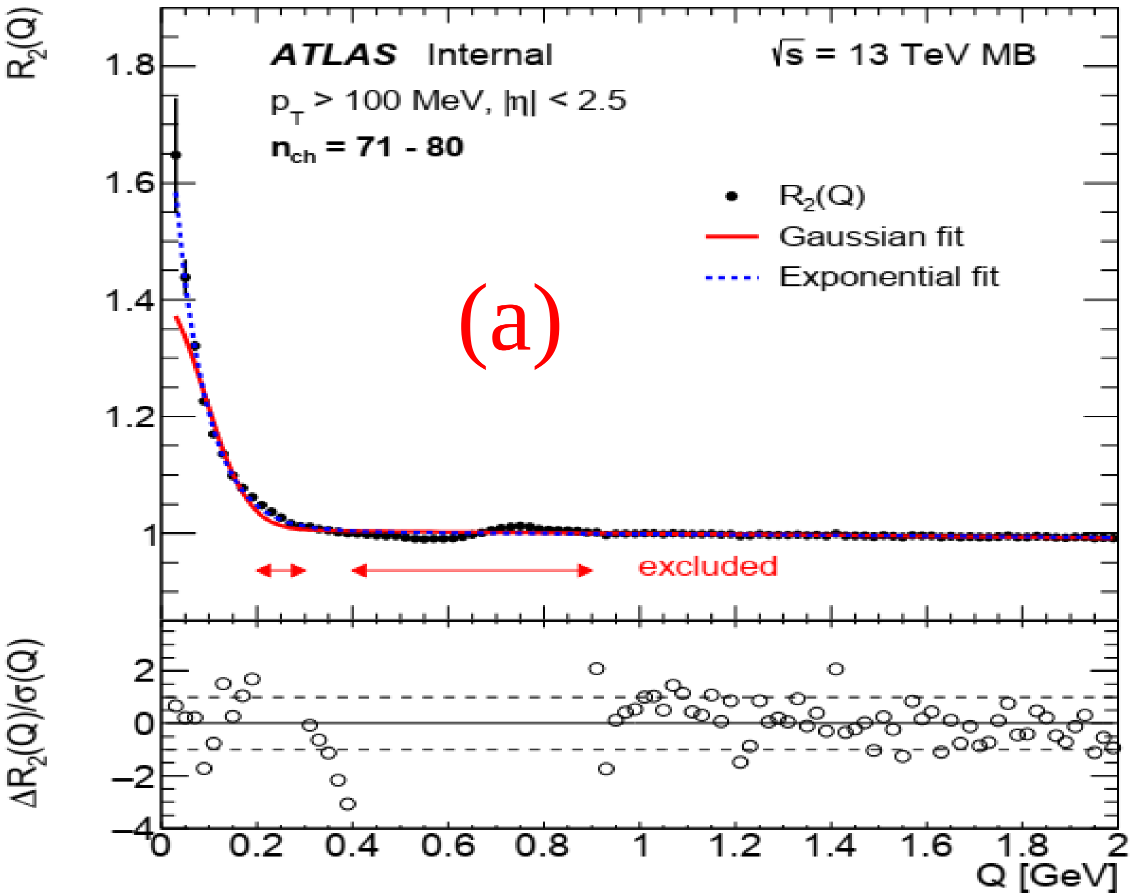

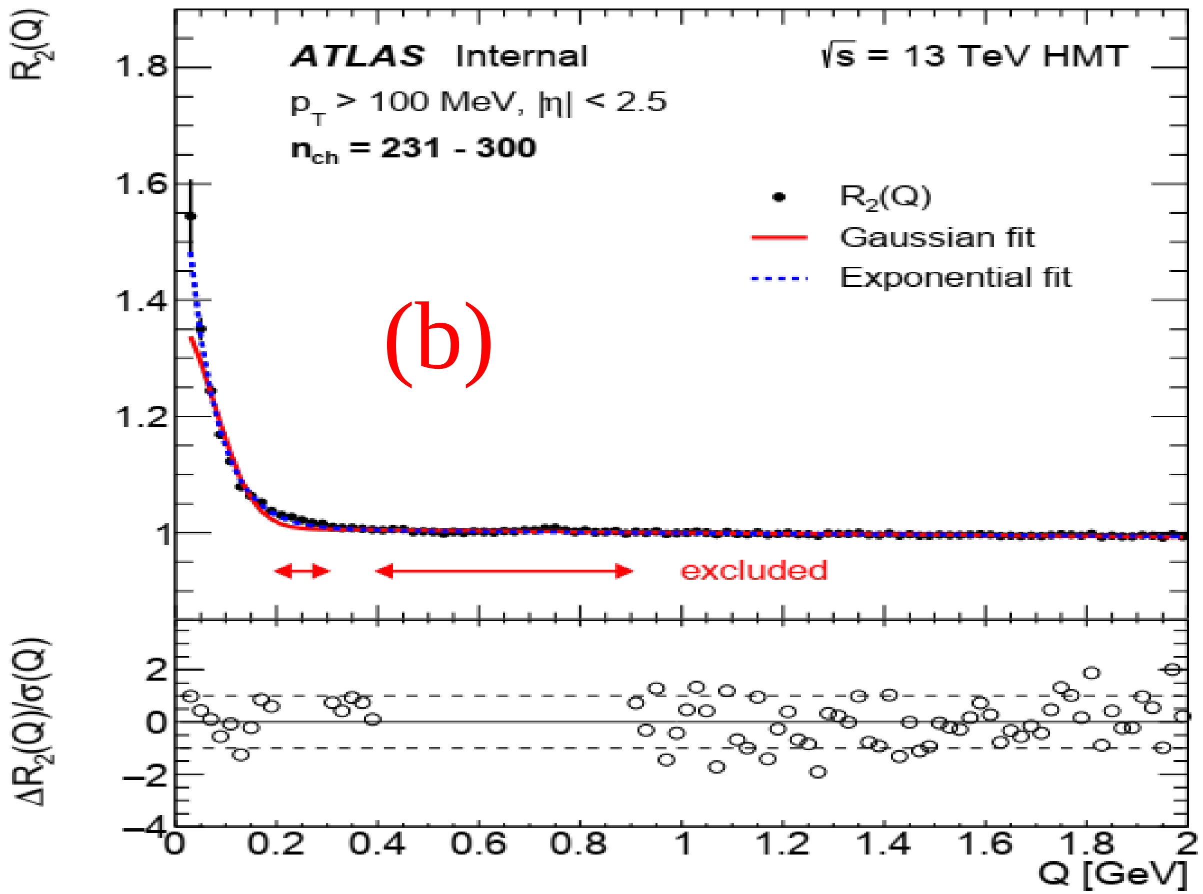

- The ***$R_2(Q)$*** for *pp* collisions for track ***p_T*>100 MeV** at 13 TeV in the multiplicity intervals
  (a) $71 \leq n_{ch} < 80$ for the MB,
  (b) $231 \leq n_{ch} < 300$ for the HMT events.
- The region excluded from the fits is shown.
- The difference between the $R_2(Q)$ and the result of the exponential fit normalized to the experimental uncertainty, $\Delta R_2(Q)/\sigma(Q)$, is presented

AVERAGE CHARGED-PARTICLE MULTIPLICITIES VS ENERGY

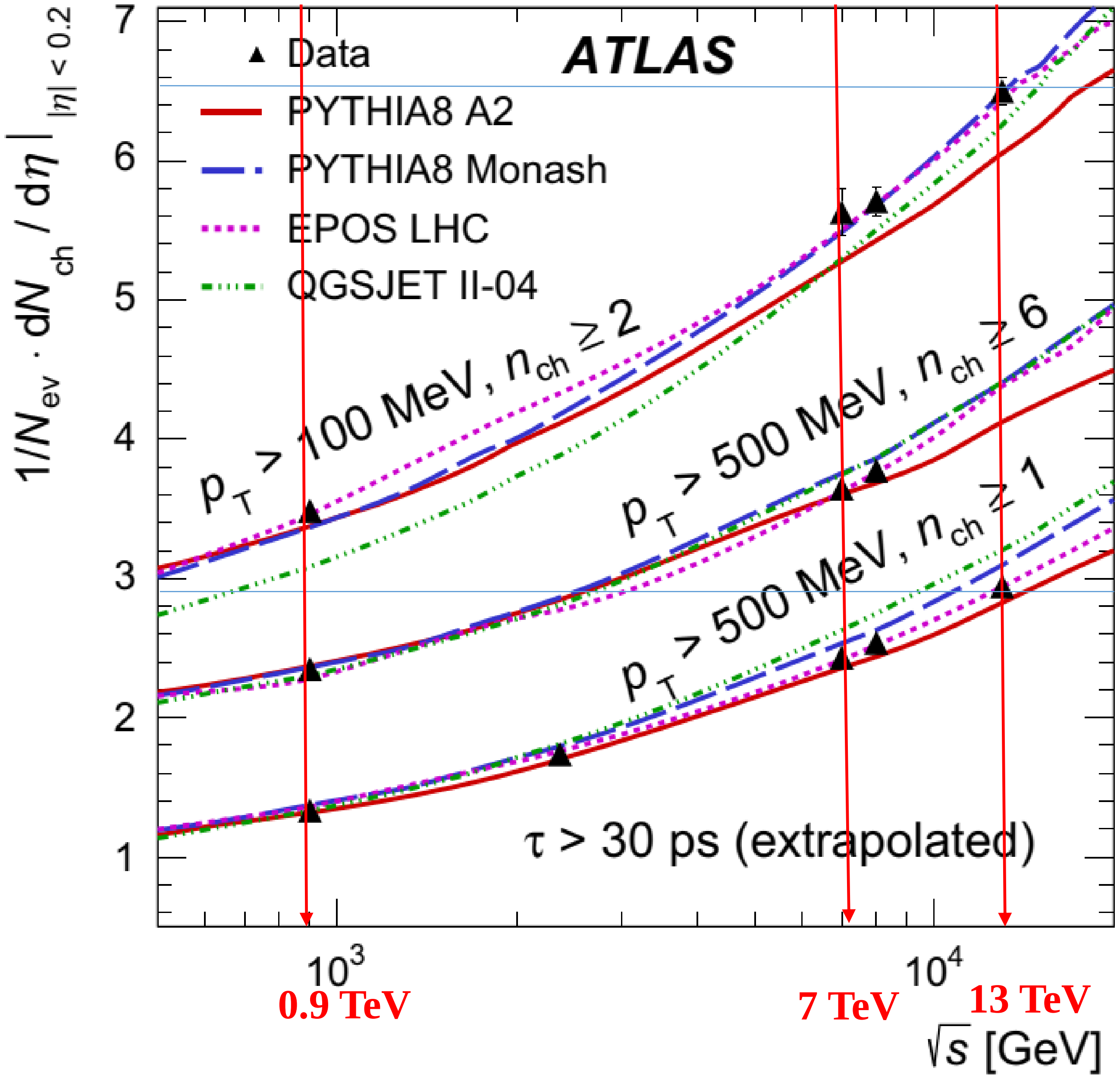

The average primary charged-particle multiplicity in *pp* interactions per unit of pseudorapidity η for $|\eta|<0.2$ as a function of the centre-of-mass energy $\sqrt{s}$. The results have been extrapolated to include charged strange baryons (charged particles with a mean lifetime of $30<\tau<300$ ps). The data are shown as *black triangles* with *vertical errors bars* representing the total uncertainty. They are compared to various MC predictions which are shown as ***coloured lines.***

$$\langle dn_{ch}/d\eta|_{|\eta|<0.2}\rangle = 1/N_{ev} \cdot dN_{ch}/d\eta|_{|\eta|<0.2}$$

$$\langle n_{ch}^{|\eta|<2.5}\rangle = 5\langle dn_{ch}/d\eta|_{|\eta|<0.2}\rangle$$

$$\boxed{m_{ch} \equiv n_{ch}/\langle n_{ch}^{|\eta|<2.5}\rangle}$$

BEC PARAMETERS VS MULTIPLICITY

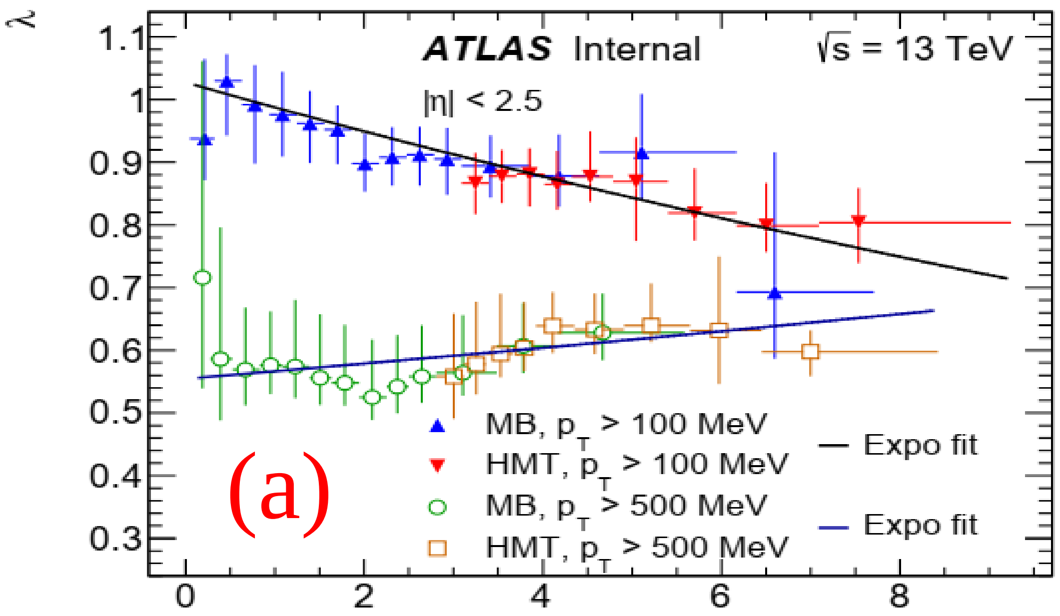

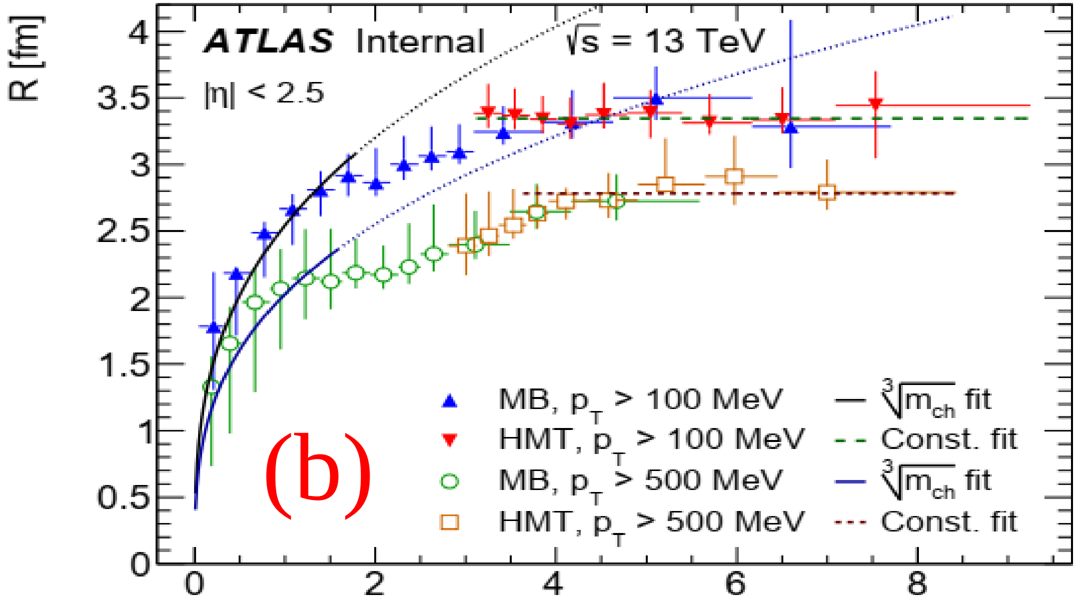

$$\boxed{m_{\mathrm{ch}} \equiv n_{\mathrm{ch}} / \langle n_{\mathrm{ch}}^{|\eta|<2.5} \rangle}$$

$$\langle n_{\mathrm{ch}}^{|\eta|<2.5} \rangle = 5 \langle dn_{\mathrm{ch}}/d\eta |_{|\eta|<0.2} \rangle$$

- The dependence of the $\lambda(m_{\mathrm{ch}})$ on rescaled multiplicity obtained from the exponential fit of the $R_2(Q)$ correlation functions for tracks with p_T>100 MeV and p_T>500 MeV at $\sqrt{s}$=13 TeV for the MB and HMT data.
- The dependence of the $R(m_{\mathrm{ch}})$ on m_{ch} and (c) on $m_{\mathrm{ch}}^{0.33}$.
- The uncertainties represent the sum in quadrature of the statistical and asymmetric systematic contributions.

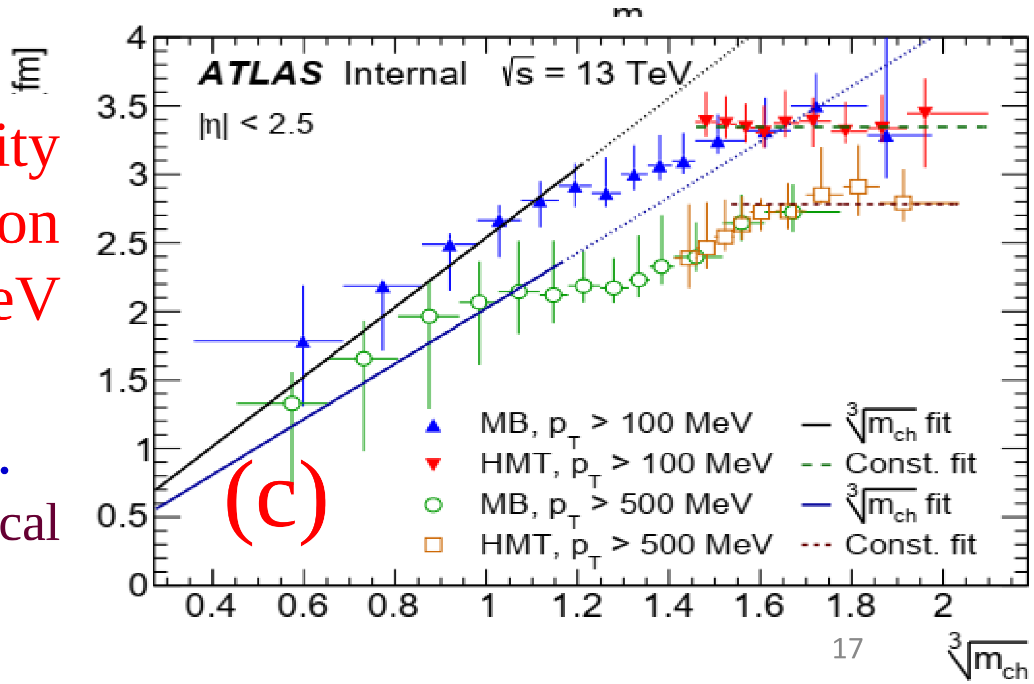

FIT RESULTS OF MULTIPLICITY DEPENDENCE OF BEC PARAMETERS

ATLAS EXPERIMENT

The results of the fits to the dependencies of the correlation strength, λ, and source radius, R, on the average rescaled charged-particle multiplicity, m_{ch}, for $|\eta|<2.5$ and both $p_T>100$ MeV and $p_T>500$ MeV at $\sqrt{s} = 13$ TeV for the MB and the HMT events. The parameters **γ and δ** resulting from a joint fit to the MB and HMT data are presented. The total uncertainties are shown.

$$\boxed{\lambda(m_{ch}) = \gamma\, e^{-\delta m_{ch}}}$$

$$\boxed{R(m_{ch}) = \alpha \sqrt[3]{m_{ch}}}$$

$$\boxed{R(m_{ch}) = \beta}$$

p_T Threshold	BEC Parameter	Fit Equation	m_{ch} Region	MB Events	HMT Events
> 100 MeV	$\lambda(m_{ch})$	(4)		$\gamma = 1.027^{+0.043}_{-0.078}$	
				$\delta = 0.039^{+0.050}_{-0.083}$	
	$R(m_{ch})$	(5)	≤ 1.9	$\alpha = 2.54^{+0.12}_{-0.22}$ fm	—
	$R(m_{ch})$	(6)	≥ 3.08		$\beta = 3.35^{+0.20}_{-0.09}$ fm
> 500 MeV	$\lambda(m_{ch})$	(4)		$\gamma = 0.555^{+0.124}_{-0.028}$	
				$\delta = -0.021^{+0.022}_{-0.007}$	
	$R(m_{ch})$	(5)	≤ 1.9	$\alpha = 2.02^{+0.29}_{-0.39}$ fm	—
	$R(m_{ch})$	(6)	≥ 4.17		$\beta = 2.78^{+0.23}_{-0.09}$ fm

Comparison of $C_2(Q)$ at 7 and 13 TeV

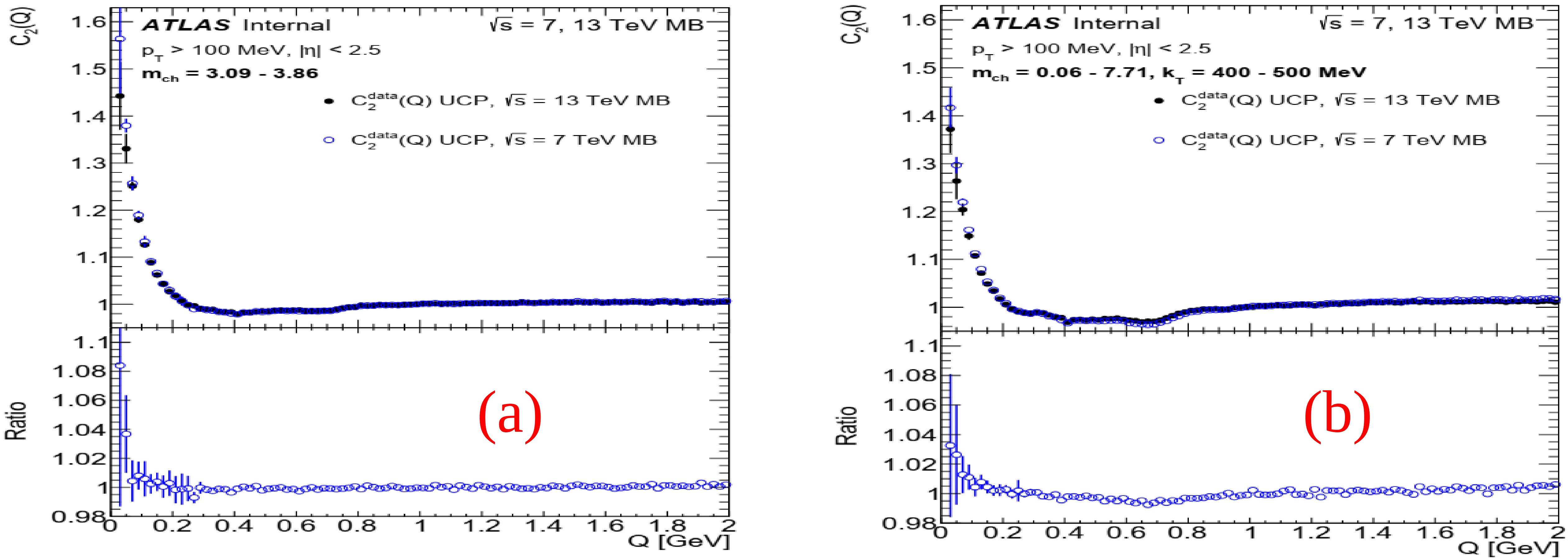

- Comparison of $C_2^{\mathbf{data}}(Q)$ correlation functions with the UCP pair reference sample for MB events (top panel) at **13 TeV (black) and 7 TeV (open blue),** and the ratio of $C_2^{7\ \mathrm{TeV}}(Q)$ **to** $C_2^{13\ \mathrm{TeV}}(Q)$ (bottom panel) are presented.
- Comparison of $C_2^{\mathbf{data}}(Q)$
  - (a) for representative multiplicity region $3.09<m_{ch}\leq3.86$ and
  - (b) for representative k_T region $400<k_T\leq500$ MeV.

k_T DEPENDENCE OF BEC PARAMETERS

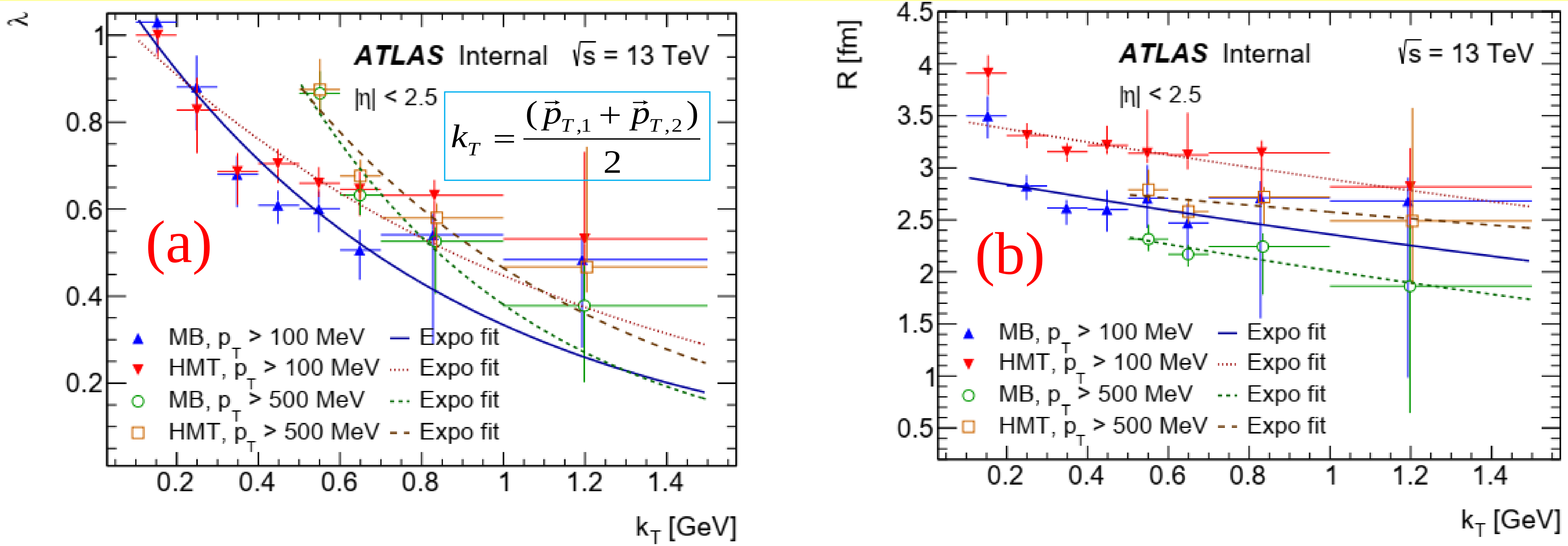

- The k_T **dependence** of (a) the correlation strength, $\lambda(k_T)$, and (b) the source radius, $R(k_T)$, obtained from the exponential fit to the $R_2(Q)$ correlation functions for tracks with p_T>100 **MeV and p_T>500 MeV at $\sqrt{s}$=13 TeV for the MB and HMT events.**
- The uncertainties represent the sum in quadrature of the statistical and systematic contributions.
- The curves represent the **exponential fits** to $\lambda(k_T)$ & $R(k_T)$.

Fit parameters of k_T dependence of BEC parameters

The results of the fits to the dependencies of the correlation strength, λ, and source radius, R, on the pair average transverse momentum, k_T, for various functional forms and for MB and HMT events for p_T>100 MeV and p_T>500 MeV at 13 TeV. The total uncertainties are shown.

$\lambda(k_T) = \mu\, e^{-\nu k_T}$

$R(k_T) = \xi\, e^{-\kappa k_T}$

BEC Parameter	Fit Equation	p_T Threshold	MB events	HMT events
$\lambda(k_T)$	(7)	> 100 MeV	$\mu = 1.18^{+0.10}_{-0.11}$	$\mu = 1.09^{+0.08}_{-0.09}$
			$\nu = 1.27^{+0.20}_{-0.30}$ GeV^{-1}	$\nu = 0.89^{+0.19}_{-0.17}$ GeV^{-1}
		> 500 MeV	$\mu = 2.10^{+0.70}_{-1.29}$	$\mu = 1.68^{+0.50}_{-0.53}$
			$\nu = 1.71^{+0.52}_{-0.92}$ GeV^{-1}	$\nu = 1.29^{+0.47}_{-0.50}$ GeV^{-1}
$R(k_T)$	(8)	> 100 MeV	$\xi = 2.98^{+0.36}_{-0.78}$ fm	$\xi = 3.51^{+0.18}_{-0.21}$ fm
			$\kappa = 0.23^{+0.29}_{-0.75}$ GeV^{-1}	$\kappa = 0.19^{+0.16}_{-0.17}$ GeV^{-1}
		> 500 MeV	$\xi = 2.71^{+0.56}_{-2.82}$ fm	$\xi = 2.92^{+0.81}_{-2.94}$ fm
			$\kappa = 0.30^{+0.38}_{-1.26}$ GeV^{-1}	$\kappa = 0.13^{+0.53}_{-68.6}$ GeV^{-1}

2-DIMENSIONAL BEC PARAMETERS

The two-dimensional surfaces for **p_T>100 MeV** & **p_T>500 MeV** for

- (a) & (c) the correlation strength, λ, and
- (b) & (d) the source radius, R,

obtained from the exponential fit to the $R_2(Q)$ correlation functions using the **MB sample** for m_{ch}≤**3.08** and the **HMT sample** for m_{ch}>**3.08**.

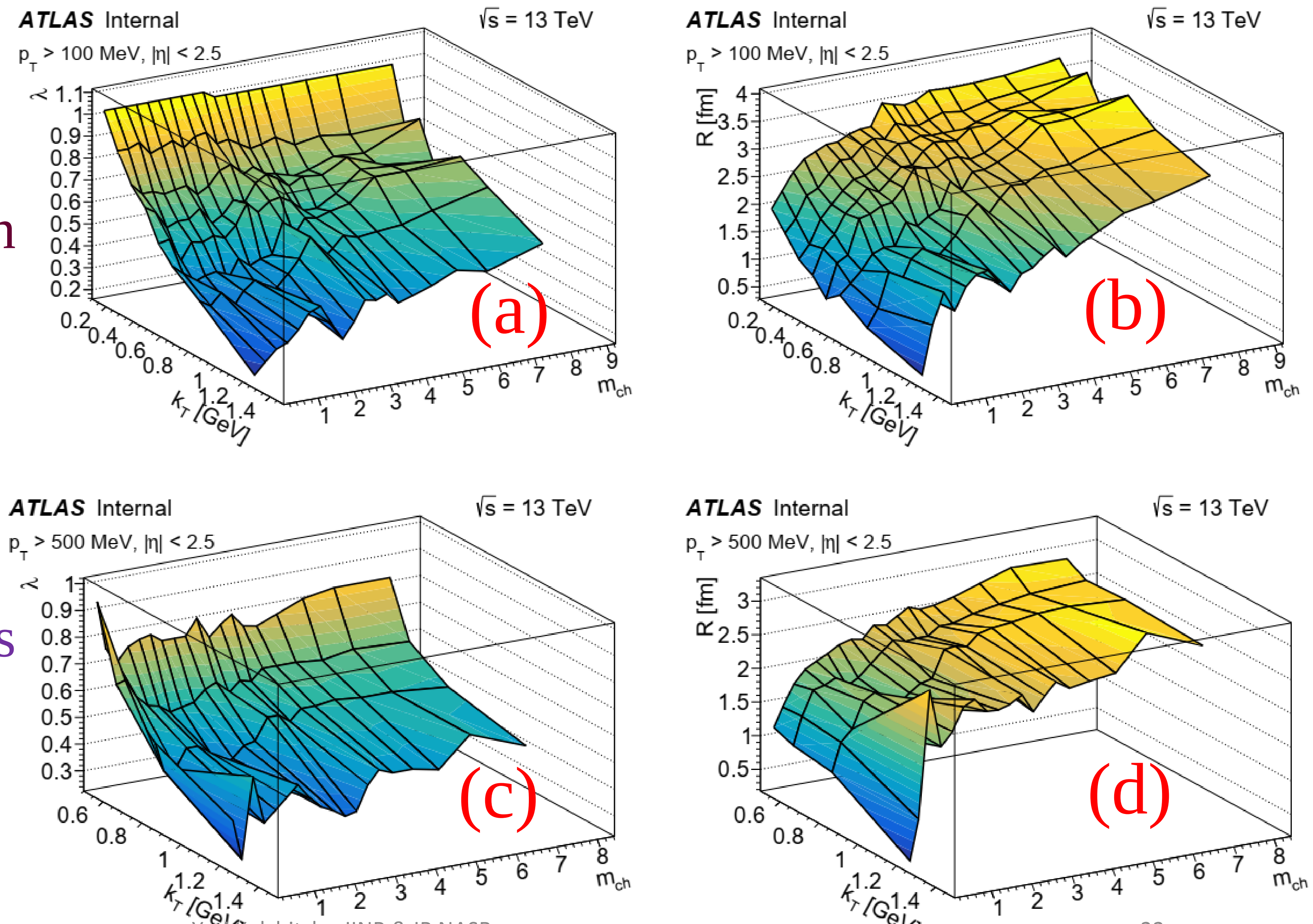

Multiplicity and k_T dependences of BEC λ-parameters for p_T>100 MeV

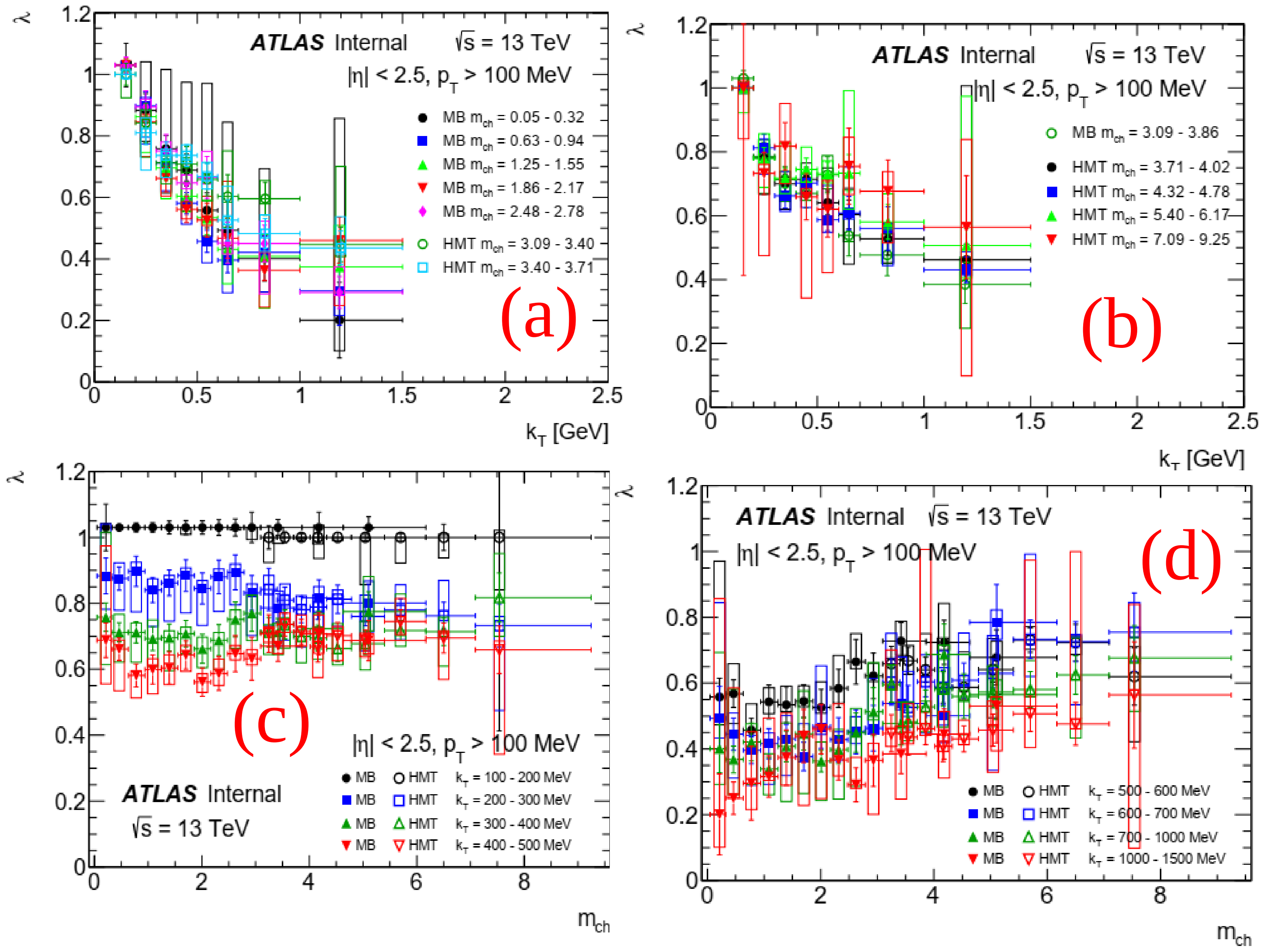

The λ for p_T>100 MeV:

(a) as a function of k_T in selected low m_{ch} intervals, (b) as a function of k_T in selected high m_{ch} intervals, (c) as a function of m_{ch} in k_T intervals between 0.1 and 0.5 GeV, (d) as a function of m_{ch} in k_T intervals between 0.5 and 1.5 GeV.

The error bars and boxes represent the statistical and systematic contributions, respectively.

MULTIPLICITY AND k_T DEPENDENCES OF BEC R-PARAMETERS FOR p_T>100 MEV

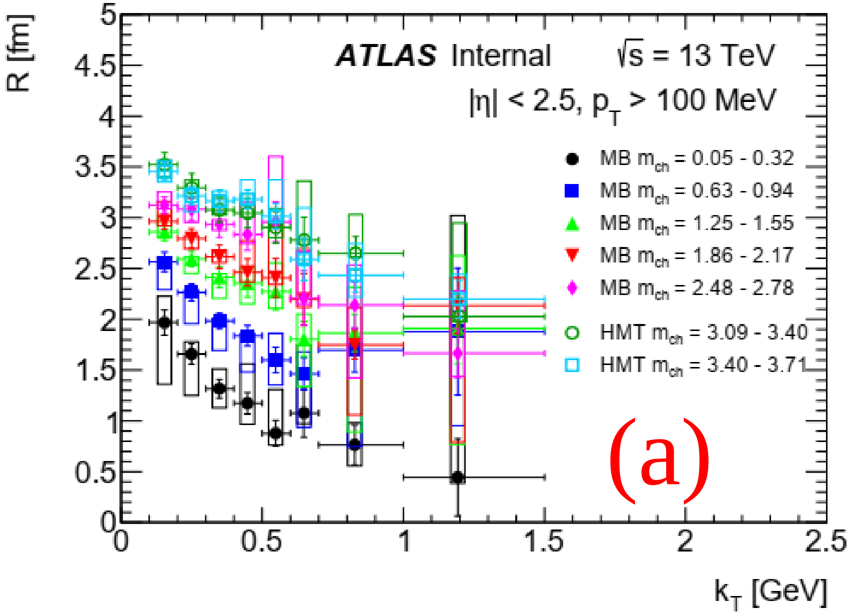

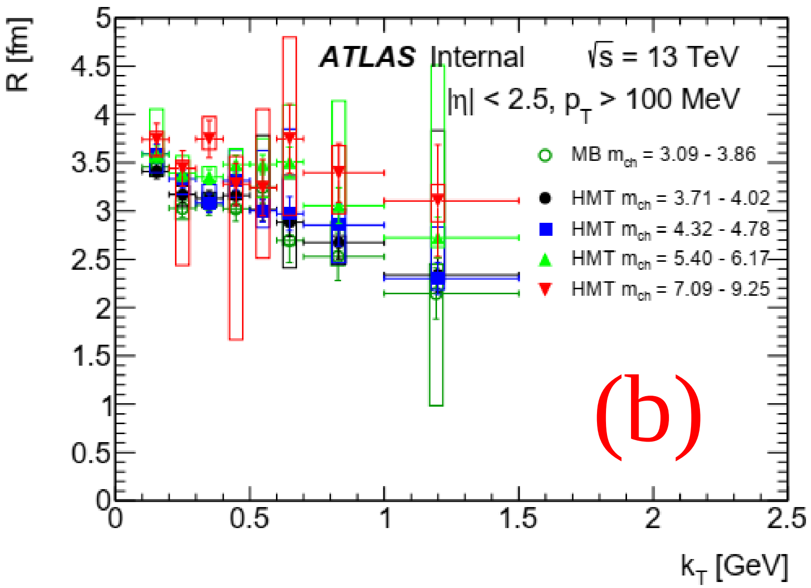

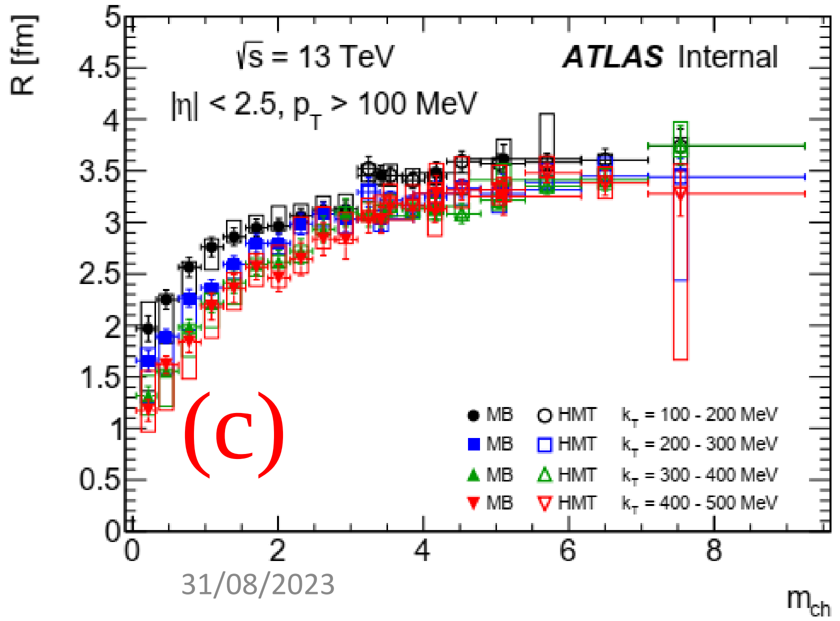

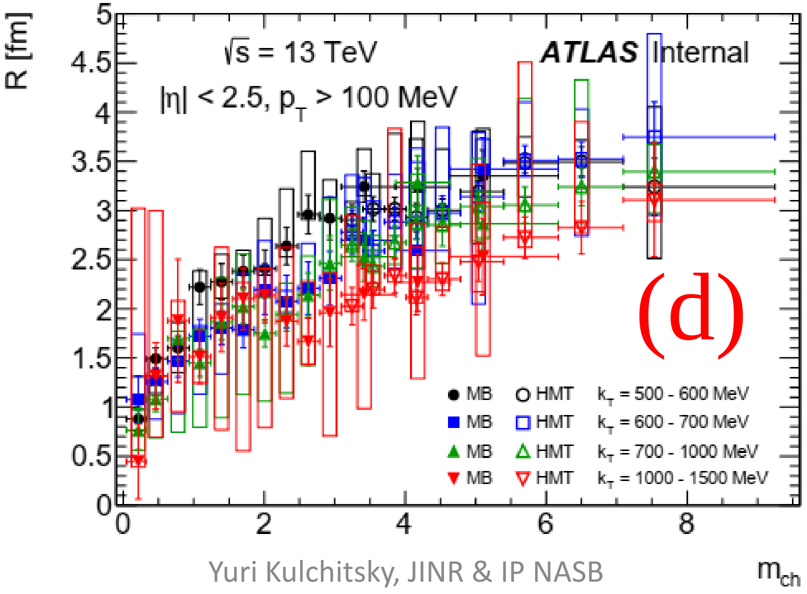

The R for p_T>100 MeV:

(a) as a function of k_T in selected low m_{ch} intervals, (b) as a function of k_T in selected high m_{ch} intervals, (c) as a function of m_{ch} in k_T intervals between 0.1 and 0.5 GeV, (d) as a function of m_{ch} in k_T intervals between 0.5 and 1.5 GeV.

The error bars and boxes represent the statistical and systematic contributions, respectively.

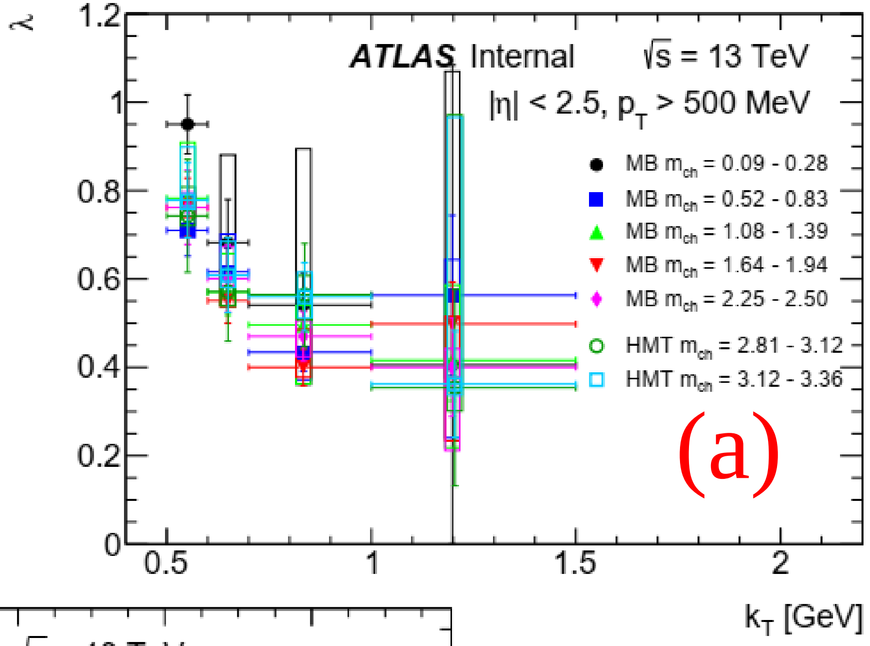

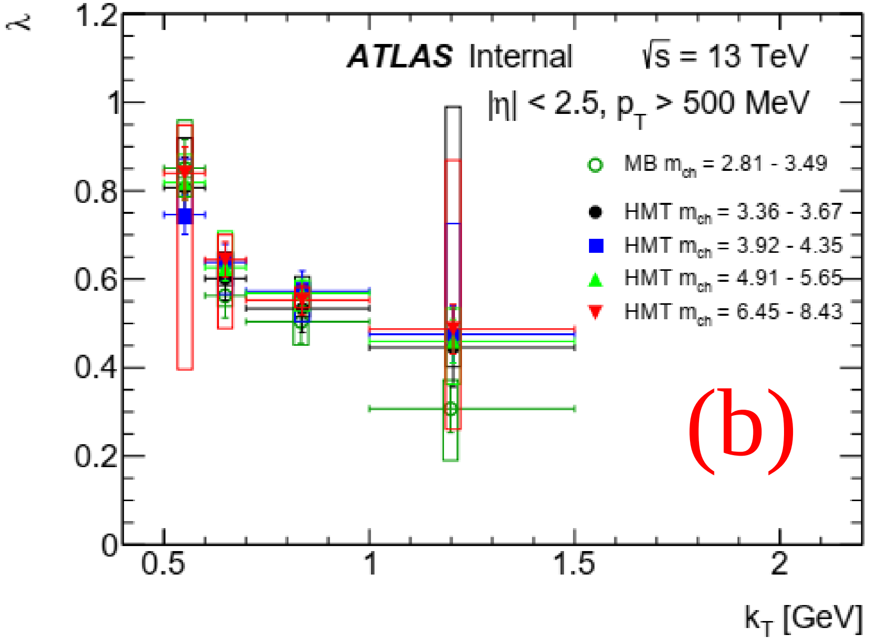

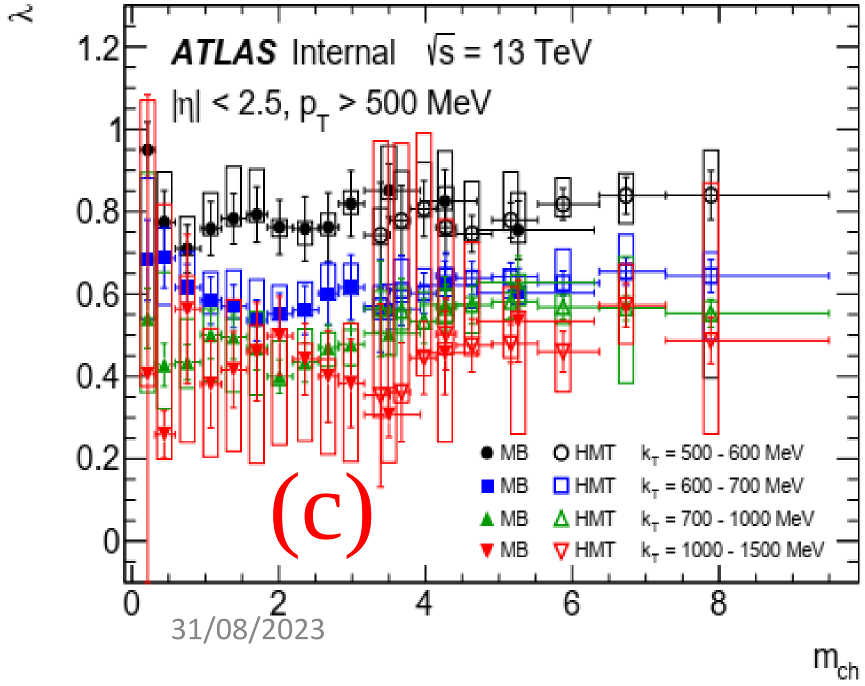

The λ for p_T>500 MeV:

(a) as a function of k_T in selected low m_{ch} intervals,
(b) as a function of k_T in selected high m_{ch} intervals,
(c) as a function of m_{ch} in k_T intervals between 0.5 and 1.5 GeV.

The error bars and boxes represent the statistical and systematic contributions, respectively.

MULTIPLICITY AND k_T DEPENDENCES OF BEC R-PARAMETERS FOR p_T>500 MEV

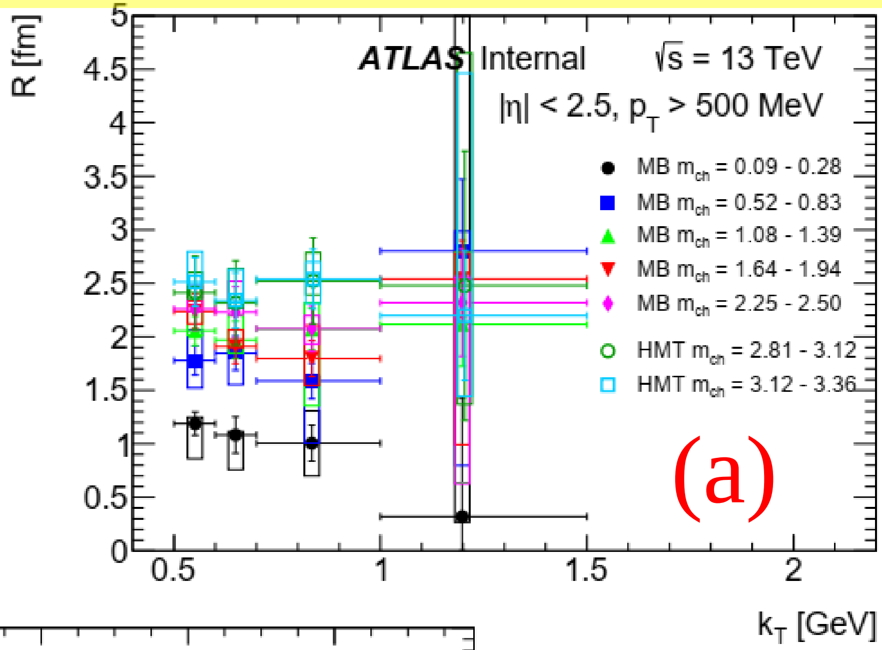

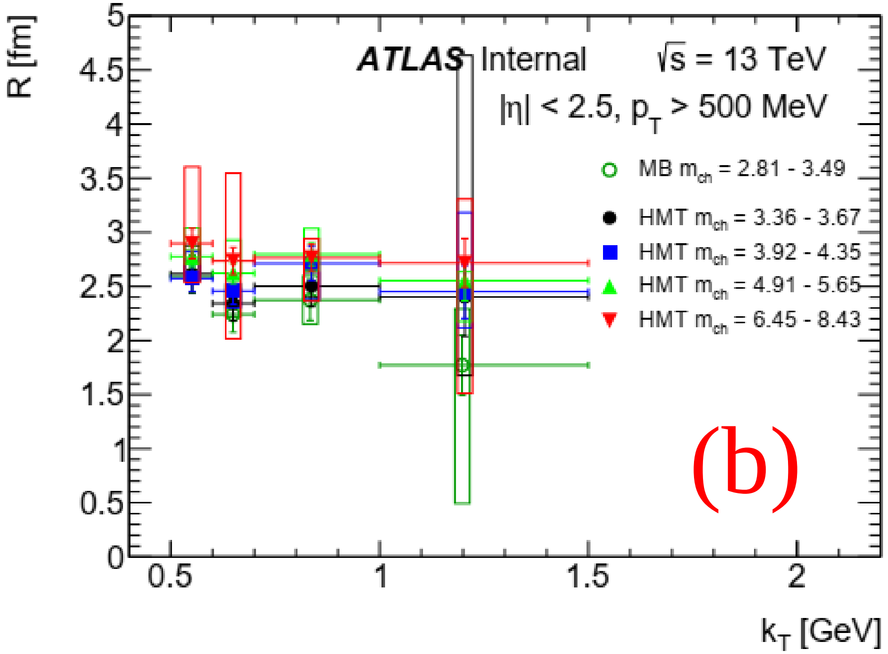

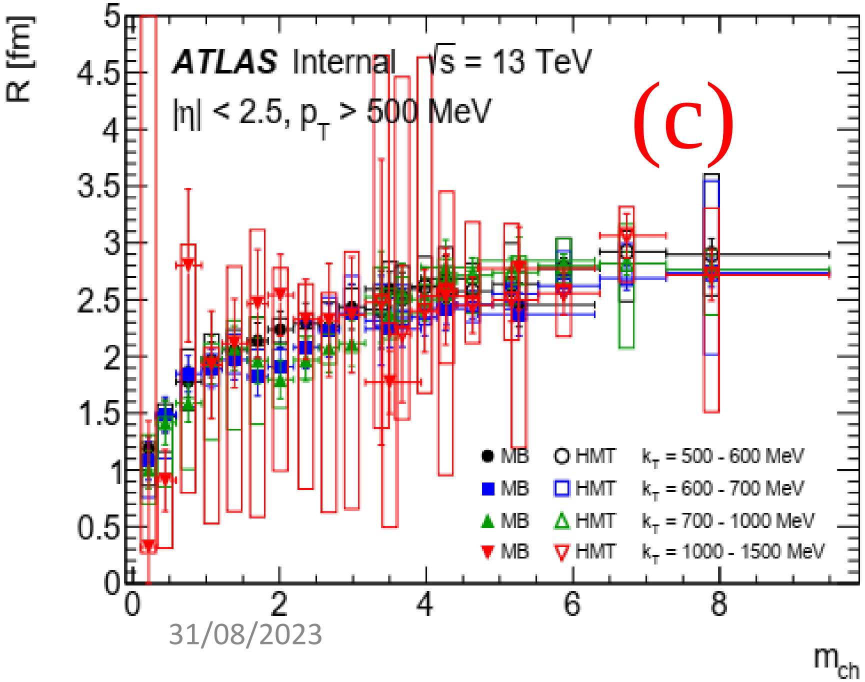

The R for p_T>500 MeV:

(a) as a function of k_T in selected low m_{ch} intervals,

(b) as a function of k_T in selected high m_{ch} intervals,

(c) as a function of m_{ch} in k_T intervals between 0.5 and 1.5 GeV.

The error bars and boxes represent the statistical and systematic contributions, respectively.

R $\langle m_{ch}\rangle$ DEPENDENCE FOR k_T FITS WITH p_T>100 & 500 MeV

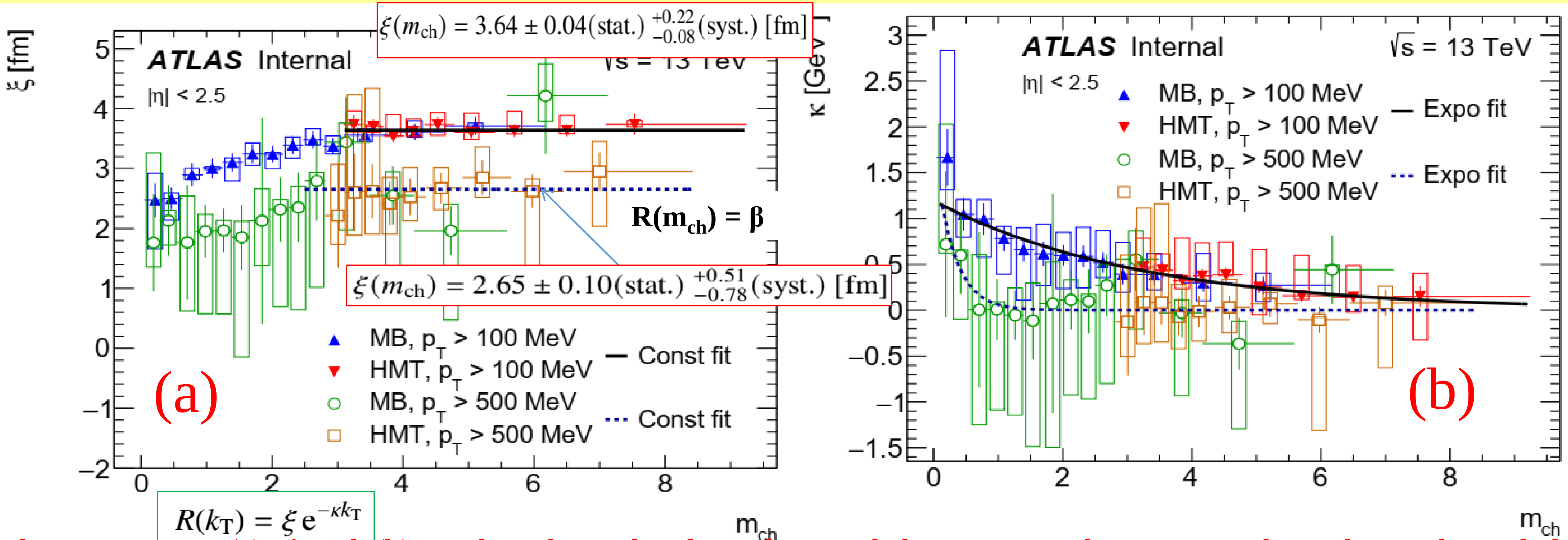

The parameters (a) ξ and (b) κ, describing the dependence of the source radius, R, on charged-particle scaled multiplicity, m_{ch}, for track p_T>100 MeV and track p_T>500 MeV in the MB and HMT samples at $\sqrt{s}$=13 TeV.

The error bars and boxes represent the statistical and systematic contributions, respectively.

(a) The black solid and blue dashed curves represent the **saturated value** of the parameter ξ for m_{ch}**>3.0** for tracks with p_T**>100 MeV** and for m_{ch}**>2.8** for tracks with p_T**>500 MeV,** respectively.

(b) (b) The black solid and blue dashed curves represent the exponential fit to the parameter κ for tracks with p_T**>100 MeV** and for tracks with p_T**>500 MeV**, respectively.

LAMBDA <M$_{CH}$> DEPENDENCE FOR K_T FITS WITH P_T>100 & 500 MEV

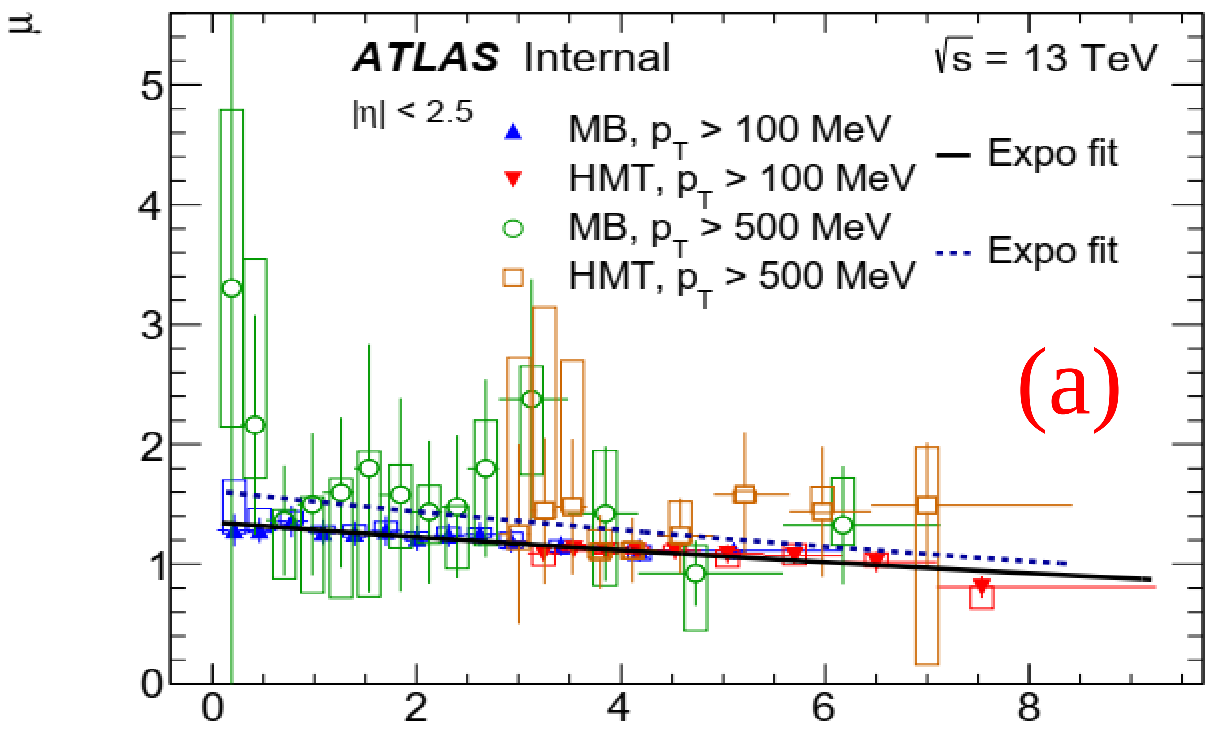

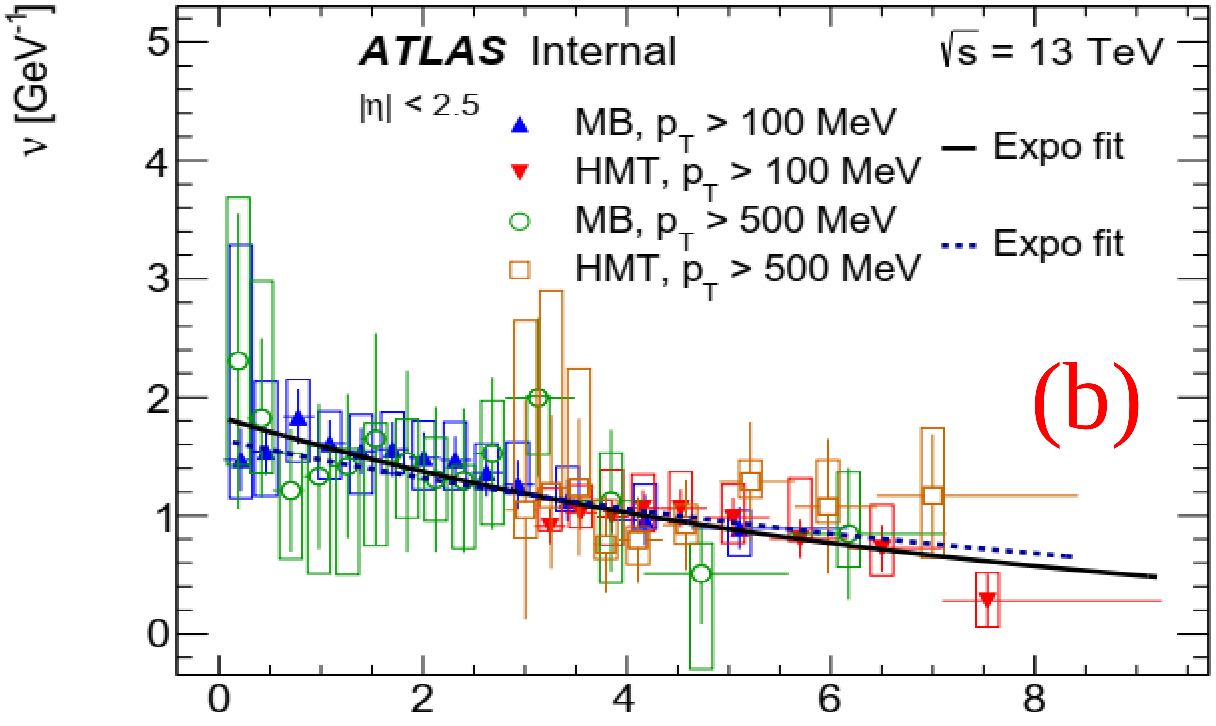

$$\lambda(k_T) = \mu\, e^{-\nu k_T}$$

$\mu(p_T$>500 MeV) > $\mu(p_T$>100 MeV) agreement in error bars

$\nu(p_T$>500 MeV) ≈ $\nu(p_T$>100 MeV)

The fit parameters (a) μ and (b) ν describing the dependence of the correlation strength, λ, on charged-particle scaled multiplicity for track p_T**>100 MeV and track** p_T**>500 MeV** in the MB and HMT samples at $\sqrt{s}$=13 TeV.

The error bars and boxes represent the statistical and systematic contributions, respectively.

The black solid (blue dashed) curve represents the exponential fit of the dependence of parameter μ (ν) **on** m_{ch} for tracks with p_T**>100 MeV** (p_T**>500 MeV**).

ATLAS & CMS BEC results comparison: n_{ch}

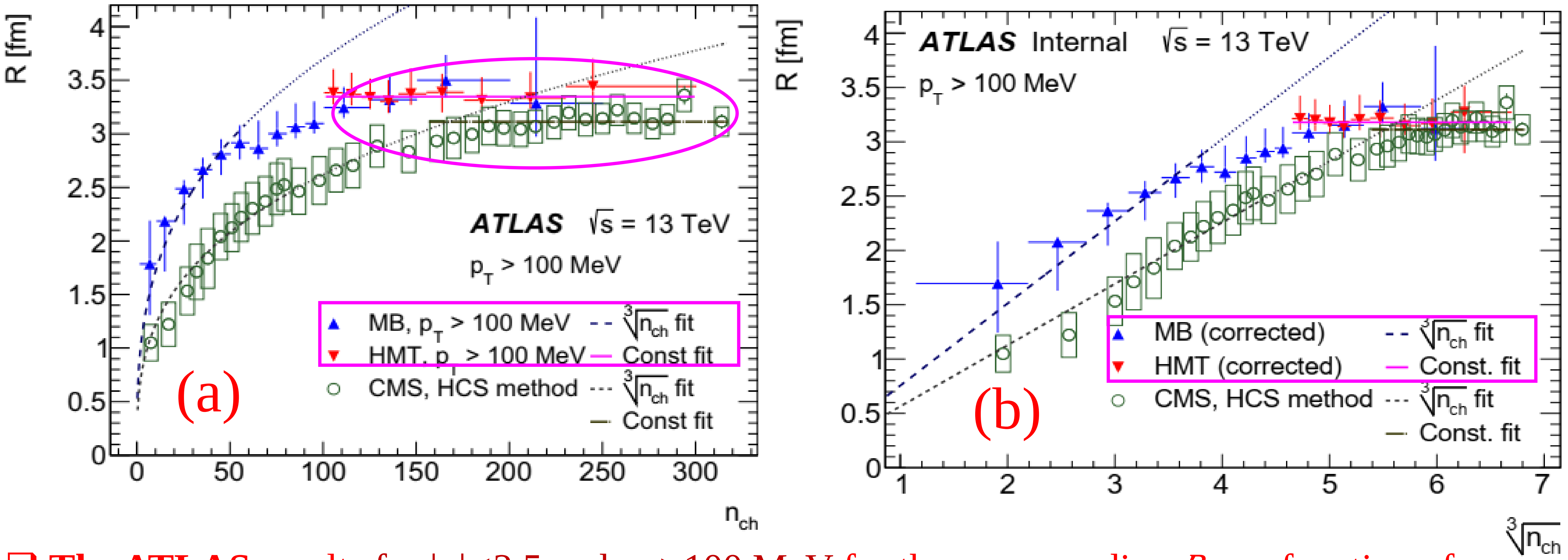

- **The ATLAS** results for $|\eta|<2.5$ and $p_T>100$ MeV for the source radius R as a function of *(a)* n_{ch} and (b) $n_{ch}^{0.33}$ in pp **interactions** at **13 TeV.**
- **The CMS** results (circles) for $|\eta|<2.4$ and rescaled to $p_T>100$ MeV.
- The ATLAS uncertainties are the sum in quadrature of the statistical and asymmetric systematic uncertainties.
- For CMS, only the systematic uncertainties are shown since the statistical uncertainties are smaller than the marker size.

ATLAS & CMS BEC RESULTS COMPARISON: k_T

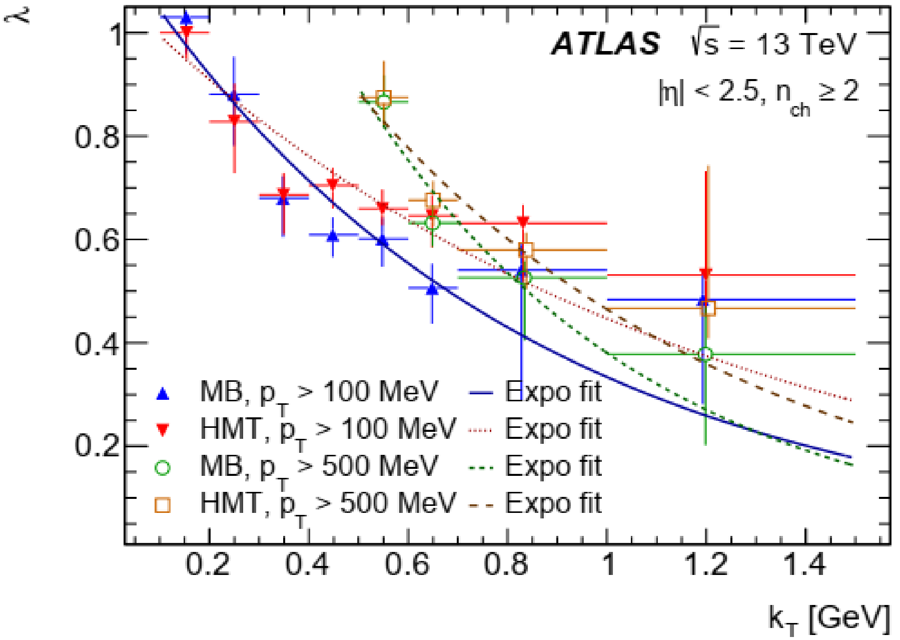

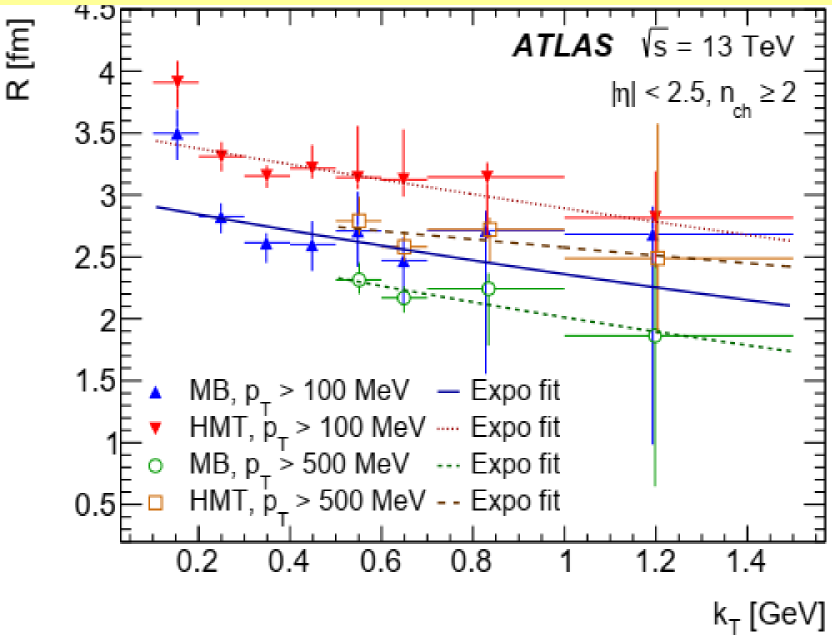

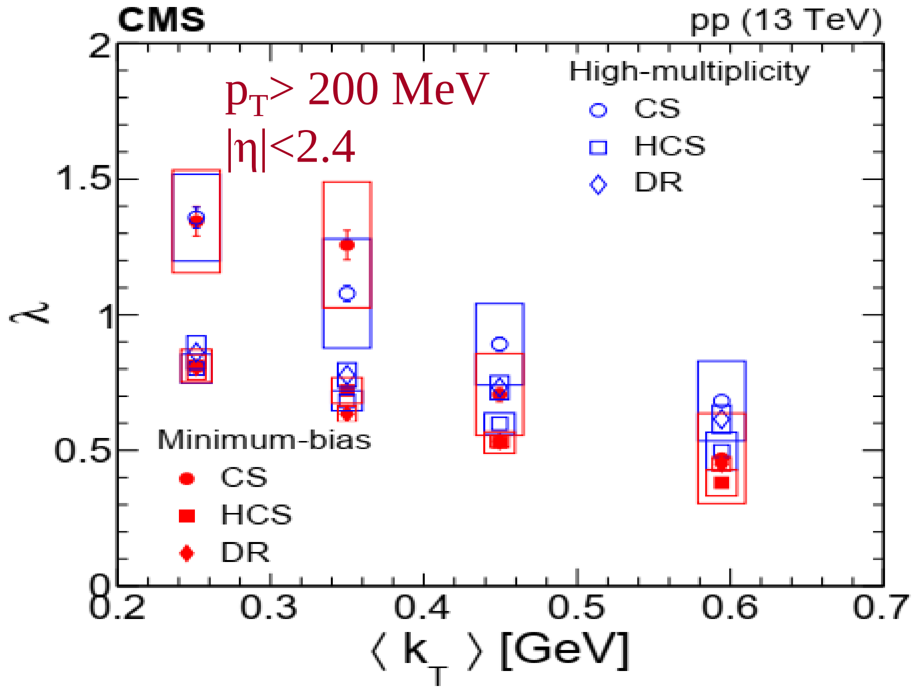

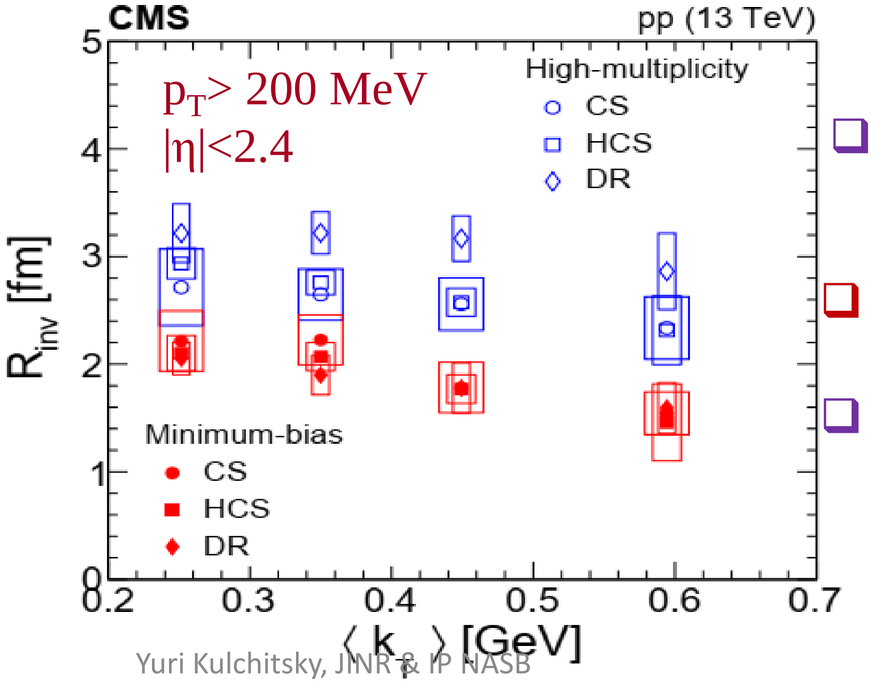

- **ATLAS:** The k_T dependence of the correlation strength, ***$\lambda(k_T)$***, and the source radius, ***$R(k_T)$***, obtained from the exponential fit to the ***$R_2(Q)$*** correlation functions for events with multiplicity ***$n_{ch} \geq 2$*** and transfer momentum of tracks with ***p_T>100 MeV*** at **13 TeV** for the minimum-bias (MB) and high-multiplicity track (HMT) events.
- The uncertainties represent the sum in quadrature of the statistical & systematic contributions.
- The curves represent the exponential fits to ***$\lambda(k_T)$* and *$R(k_T)$***.

- **CMS**: Results for **R_{inv} and λ from** the three methods as a function of k_T
- In the lower plots, statistical & systematic uncertainties are shown as error bars and open boxes, respectively

CONCLUSIONS

- The two-particle BEC of like-charge hadrons with track p_T-thresholds of 100 and 500 MeV and $|\eta|<2.5$ produced in pp collisions at $\sqrt{s}$=13 TeV recorded by the ATLAS detector at the LHC are presented. The study is carried out using data collected with the MB and HMT triggers.
- The BEC parameters, R and λ, are studied as functions of a scaled charged-particle multiplicity m_{ch}, the pair average transverse momentum (k_T) and in (m_{ch},k_T)-intervals.
- The parameter $R(m_{ch})$ is found to increase as $\alpha m_{ch}^{0.33}$ for low multiplicity for p_T thresholds. For p_T>100 MeV, $\alpha=2.54^{+0.12}_{-0.22}$ **fm**, for scaled multiplicity up to $m_{ch} \approx 2$.
- **For $m_{ch} \geq 3$**, the source radius R **saturates at a value $R = 3.35^{+0.20}_{-0.09}$ fm**, confirming the previous observation of a high-multiplicity plateau by ATLAS at $\sqrt{s}$ =7 TeV. For p_T>500 MeV, the behaviour of R is similar and lower.
- The **parameter $\lambda(m_{ch})$ decreases with multiplicity for the lower p_T threshold** and **is lower** for the higher p_T threshold **but increases slightly with multiplicity.**
- **The parameters $R(k_T)$ and $\lambda(k_T)$ both decrease with increasing pair average transverse momentum k_T.**
- The radius parameter R **also decreases with k_T for p_T>100 MeV, decreasing more strongly** in the lower m_{ch} intervals. For p_T>500 MeV the behaviour of R is rather flat with k_T. As a function of m_{ch}, R increases and reaches a plateau at large multiplicity in all m_{ch} intervals and for both p_T thresholds.
- A comparison of the R parameter as a function of m_{ch} with CMS results at 13 TeV shows similar behaviour

THANK YOU VERY MUCH FOR ATTENTION!

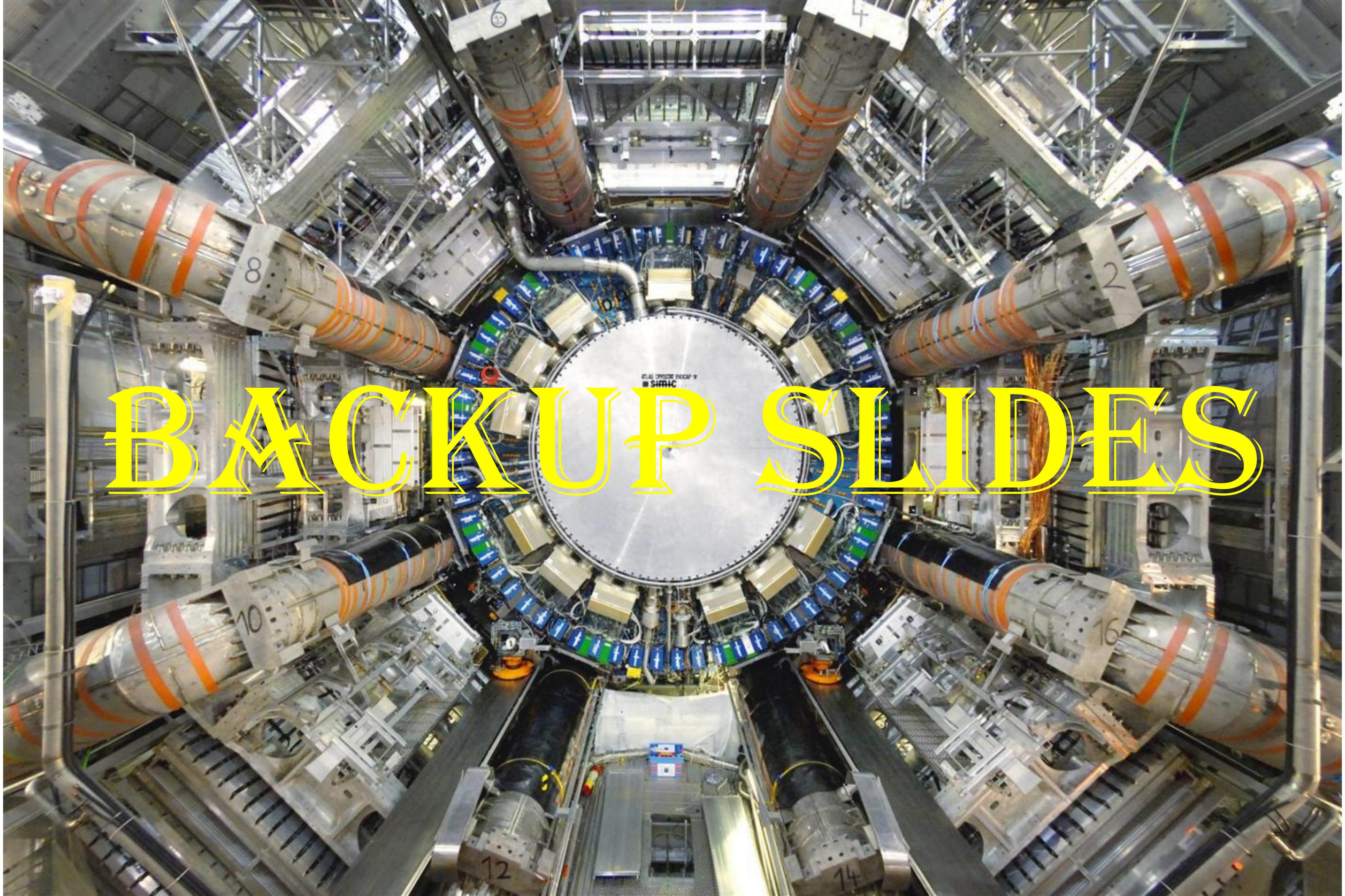

BACKUP SLIDES

EVENT CORRECTIONS

We correct the events on:

$$w(n) = \frac{1}{\varepsilon_{trig}(n) \cdot \varepsilon_{vert}(n)}$$

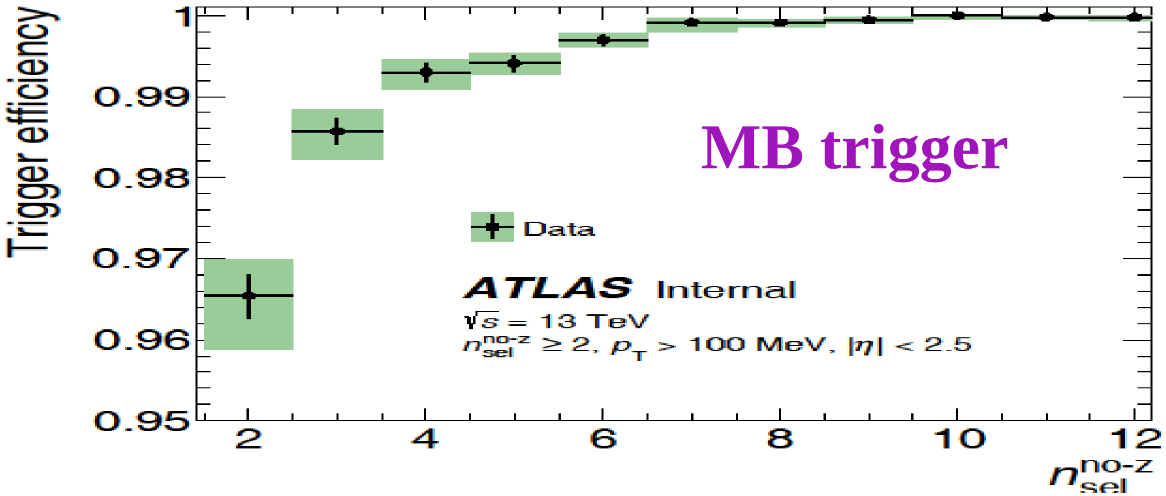

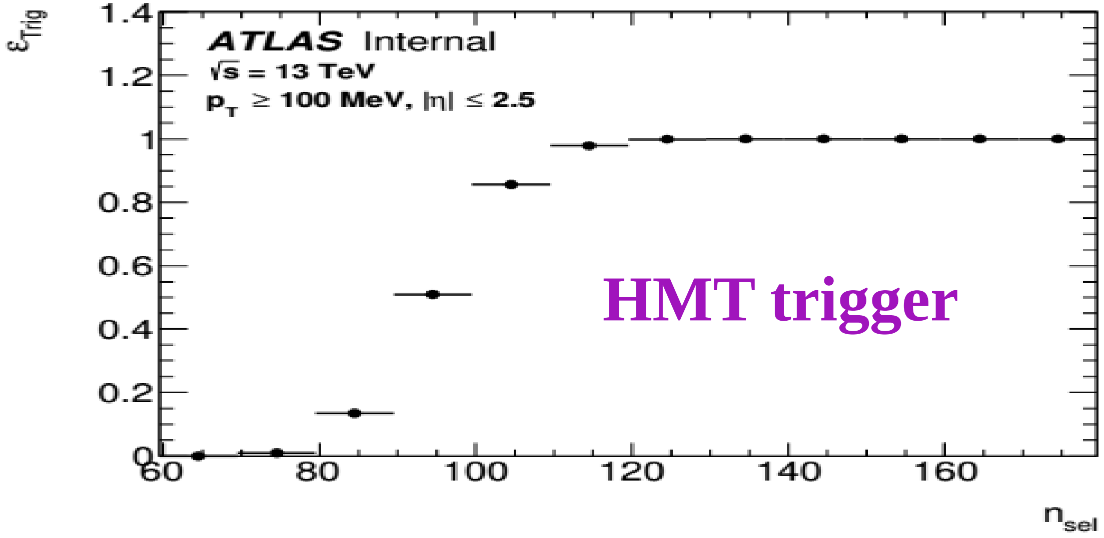

The MB or HMT triggers efficiency, $\varepsilon_{trig}(n)$

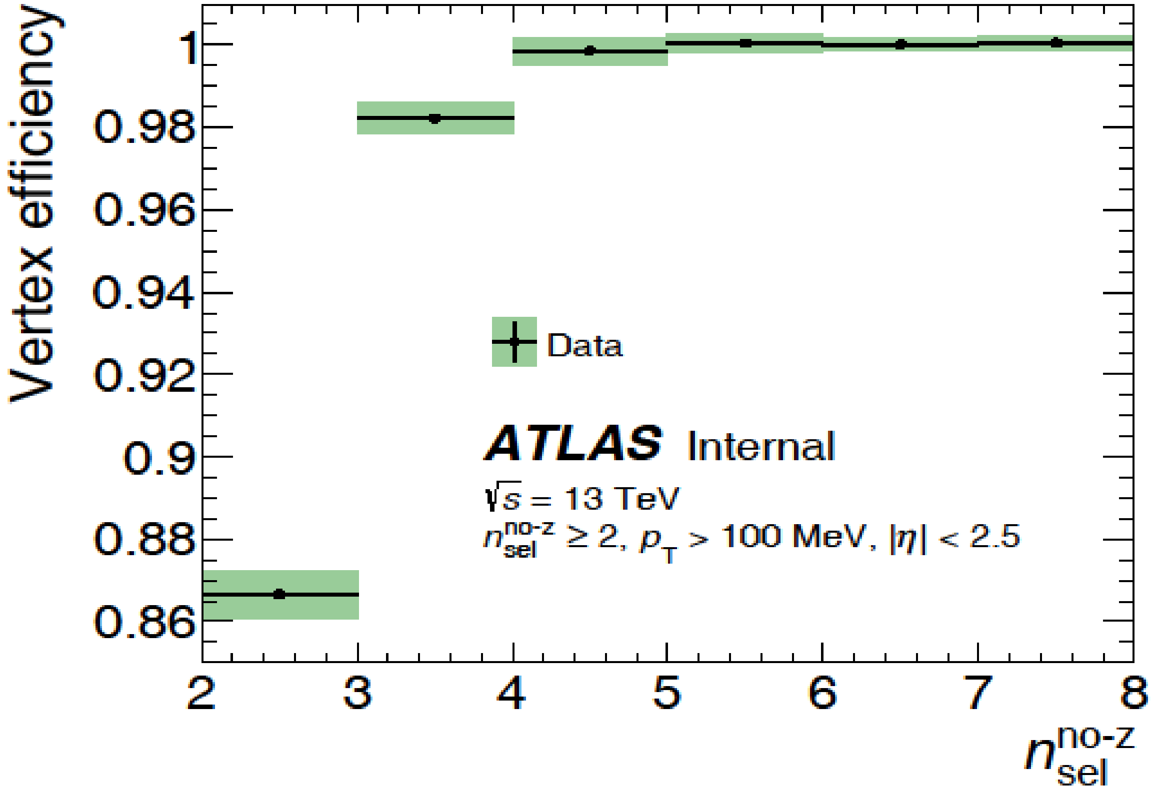

The vertex reconstruction efficiency, ε_{vert} (n)

Minimum-bias event selection criteria

Events pass the data quality criteria. "Good events":

- **all ID sub-systems nominal conditions,**
- **stable beam,**
- **defined beam spot**

- **Trigger:**
  - Accept on signal-arm Minimum Bias Trigger Scintillator for minimum-bias or high multiplicity track triggers
- **Vertex:**
  - Primary vertex (2 tracks with p_T>100 MeV),
  - Veto to any additional vertices with ≥4 tracks,
- **Tracks:** At least 2 tracks with p_T>100 MeV, $|\eta|<2.5$;
  - At least 1 first Pixel layer hit;
  - At least 2, 4, or 6 SCT hits for p_T>100, 300, 400 MeV respectively;
  - IBL hit required if expected (if not expected, next to innermost hit required if expected);
  - Cuts on the transverse impact parameter: $|d_0^{BL}|<1.5$ mm (w.r.t beam line);
  - Cuts on the longitudinal impact parameter: $|\Delta z_0 \sin\Theta|<1.5$ mm, where Δz_0 is difference between z_0^{tracks} & z^{vertex};
  - Track fit χ^2 probability >0.01 for tracks with p_T>10 GeV.

Correct distributions for detector effects:

- where possible the data used to reduce the MC dependencies
- Monte Carlo derived corrections for tracking

TRACK RECONSTRUCTION CORRECTIONS

Performed corrections on:

1. The reconstruction track efficiency – ε (p_T,η),
2. The fraction of non-primary (secondaries and fake) tracks – $f_{nonp}(p_T,\eta)$,
3. The fraction of tracks for which the corresponding primary particles are outside the kinematic range – $f_{okr}(p_T,\eta)$,
4. The strange barion tracks – $f_{sb}(p_T,\eta)$,

We use the formula, **as in MB studies**:

$$w_i\,(pT,\eta) = \frac{(1 - fnonp(p_T,\eta) - fokr(p_T,\eta) - fsb(p_T,\eta))}{\varepsilon(p_T,\eta)}$$

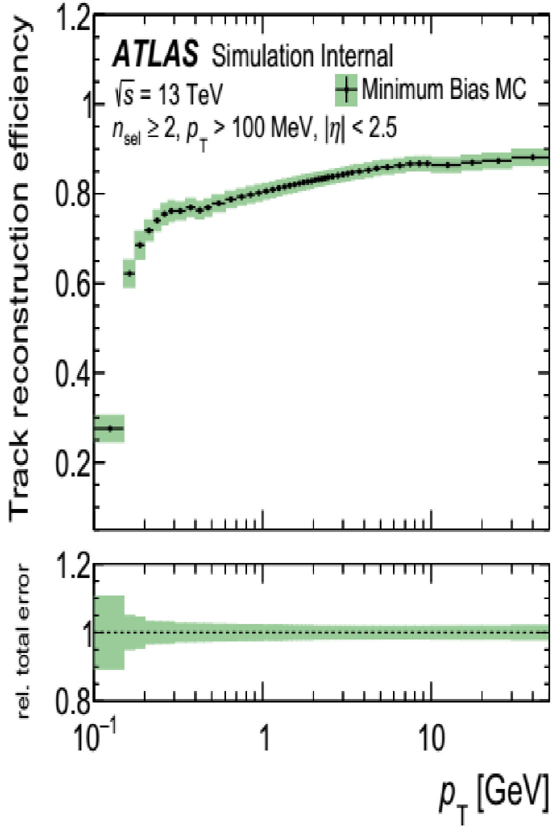

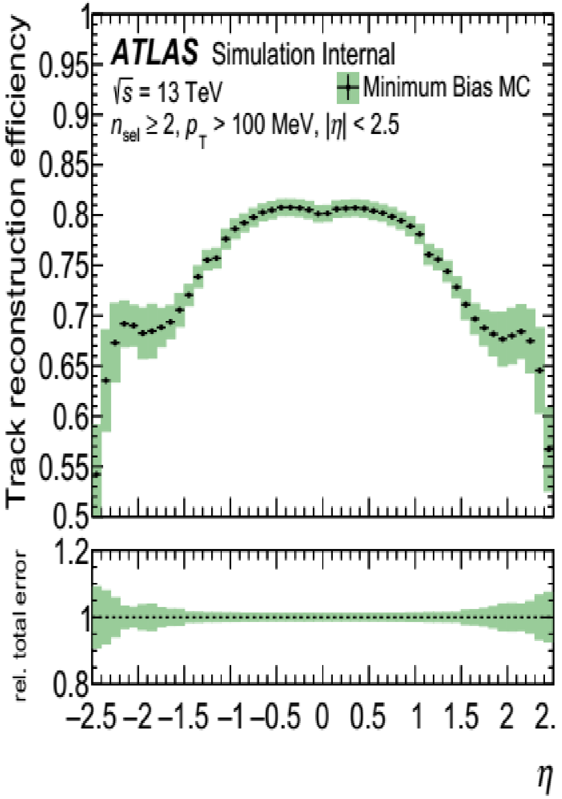

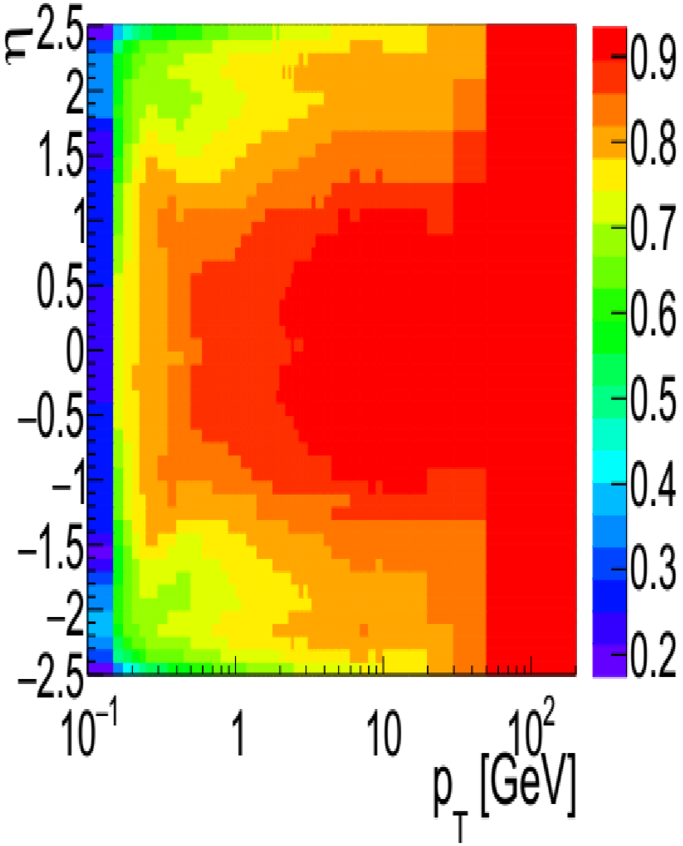

The primary track reconstruction efficiency integrated over p_T (left), integrated over η (middle) and as function of p_T and η (right). The green shaded error band includes the total systematic and statistical uncertainty

The Phase Space Correction

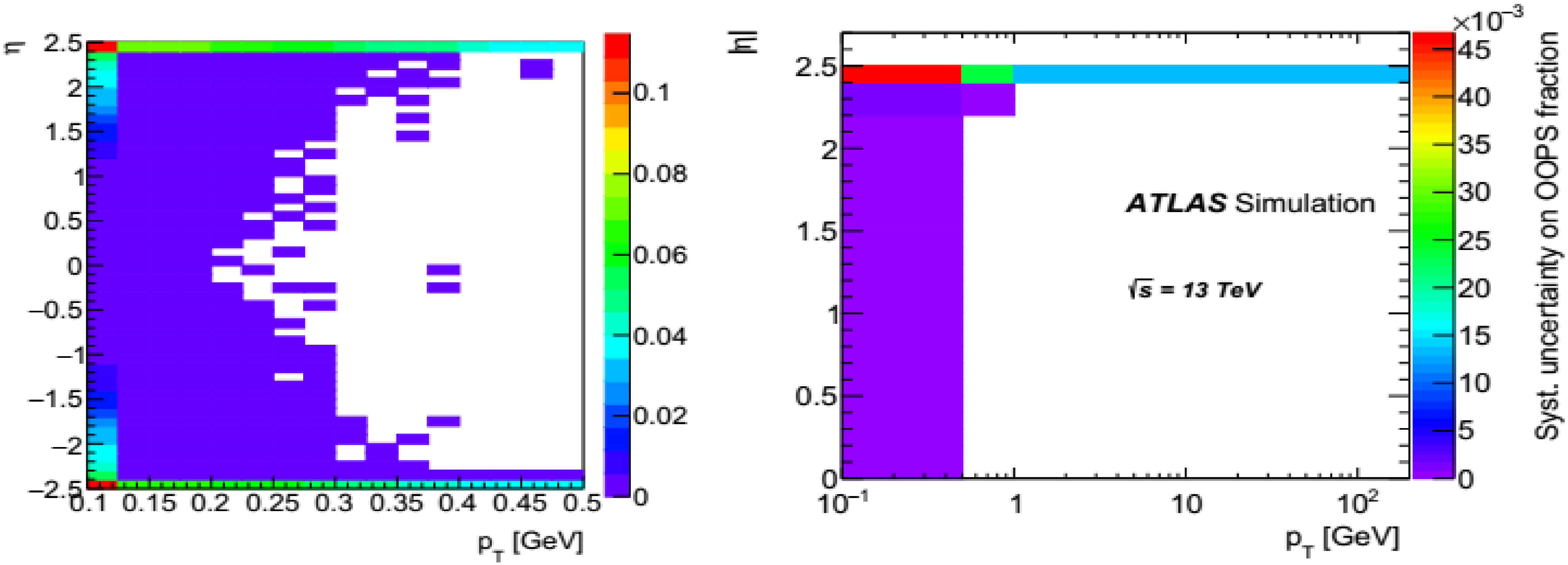

Figure 16: The out of phase space correction (OOPS) in p_T and η bins (left) and the systematic uncertainty on the out of phase space correction fractions (b). The systematic is made up of several contributions added up in quadrature, where each contribution is calculated as the difference in migration fractions between samples (see body text for further explanation).

PILE-UP FOR HMT AND MB EVENTS

MB trigger

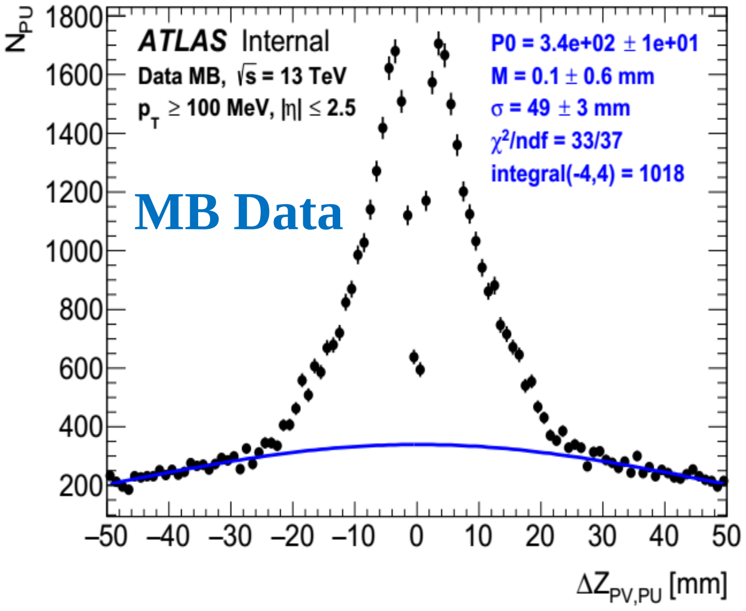

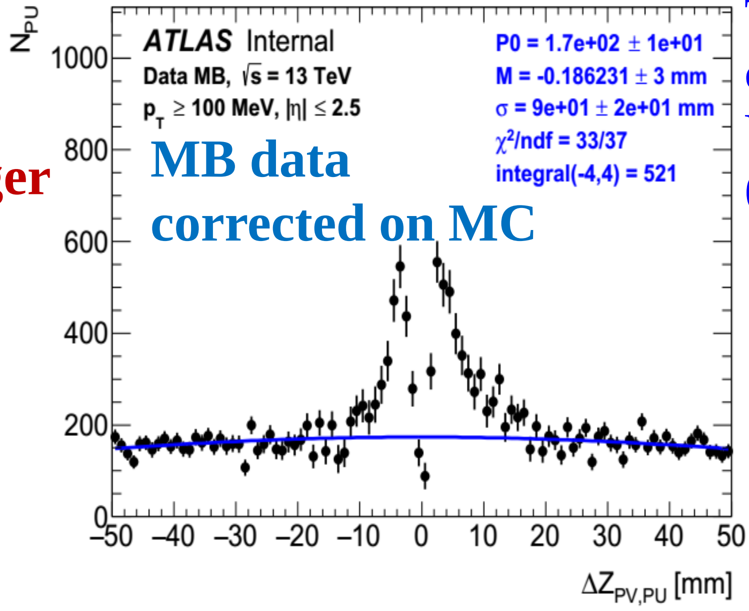

The distribution of the distance between Z coordinates of Primary Vertex and Pile-Up Vertexes for MB and HMT events for Data (left) and Data corrected on MC (right)

For MB events the number of pile-up vertexes in the Primary Vertex (PV) region ±4 mm is ~520 after correction on MC, and the number of tracks in Pile-up vertex is 9.4. Therefore the fraction of pile-up tracks in MB events is **0.002%**

HMT trigger

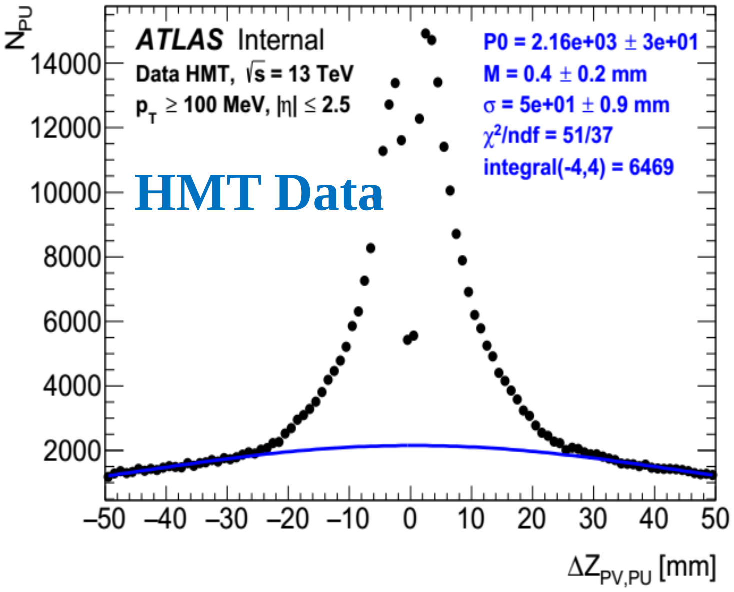

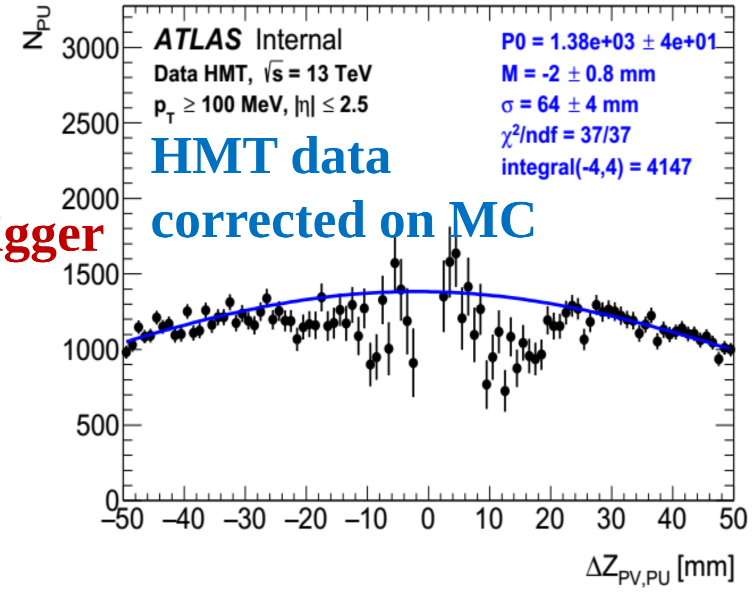

For HMT events the number of pile-up vertexes in the Primary Vertex (PV) region ±4 mm is ~4150, after correction on MC, and the number of tracks in Pile-up vertex is 23. Therefore the fraction of pile-up tracks in MB events is **0.01%**

We can conclude that mean number of pile-up tracks per MB or HMT event is negligible

Mean number of tracks (pile-up tracks) per event: MB – 26 (0.0005) tracks/event; HMT – 108 (0.01) tracks/event

MULTIPLICITY UNFOLDING FROM MB ANALYSIS

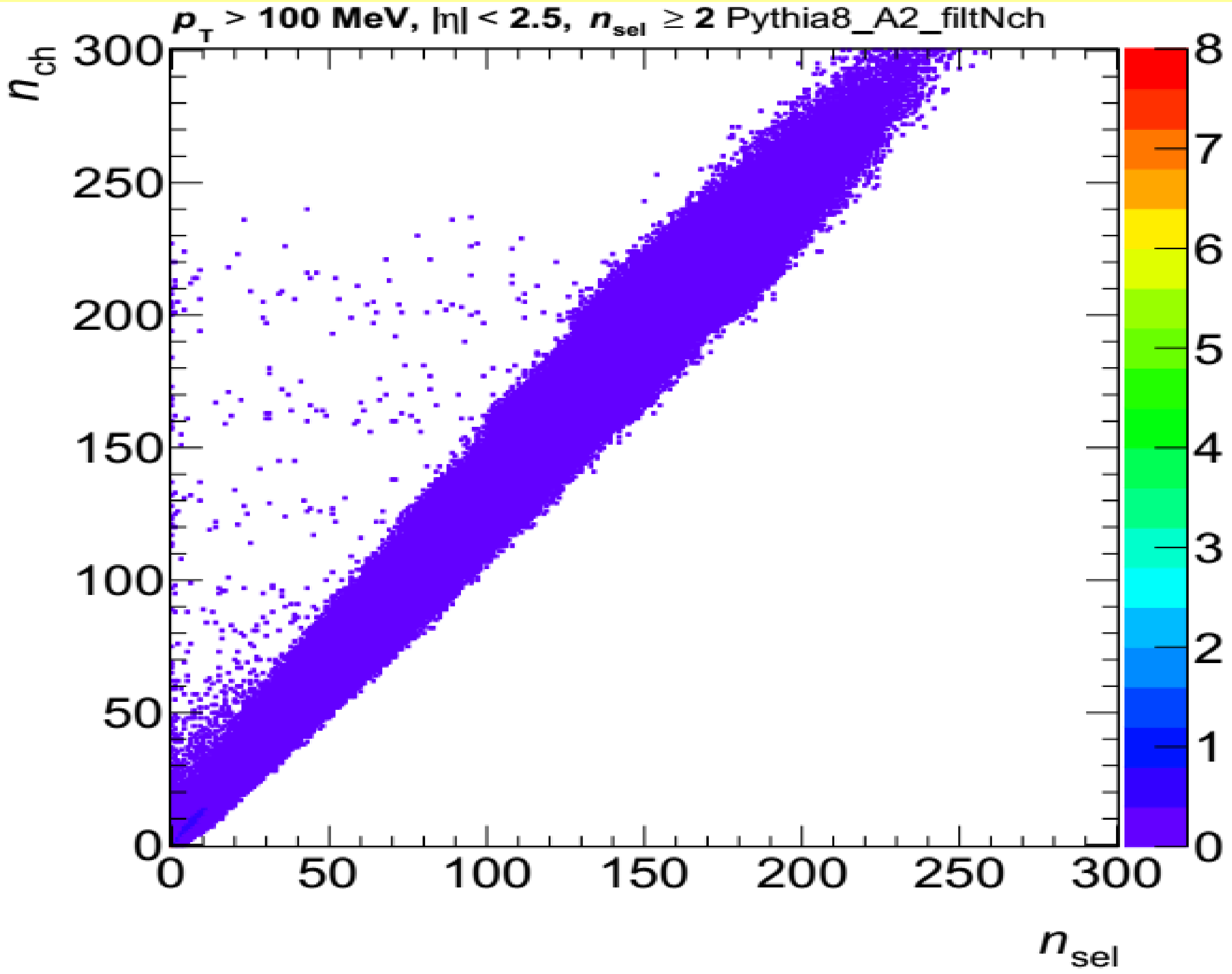

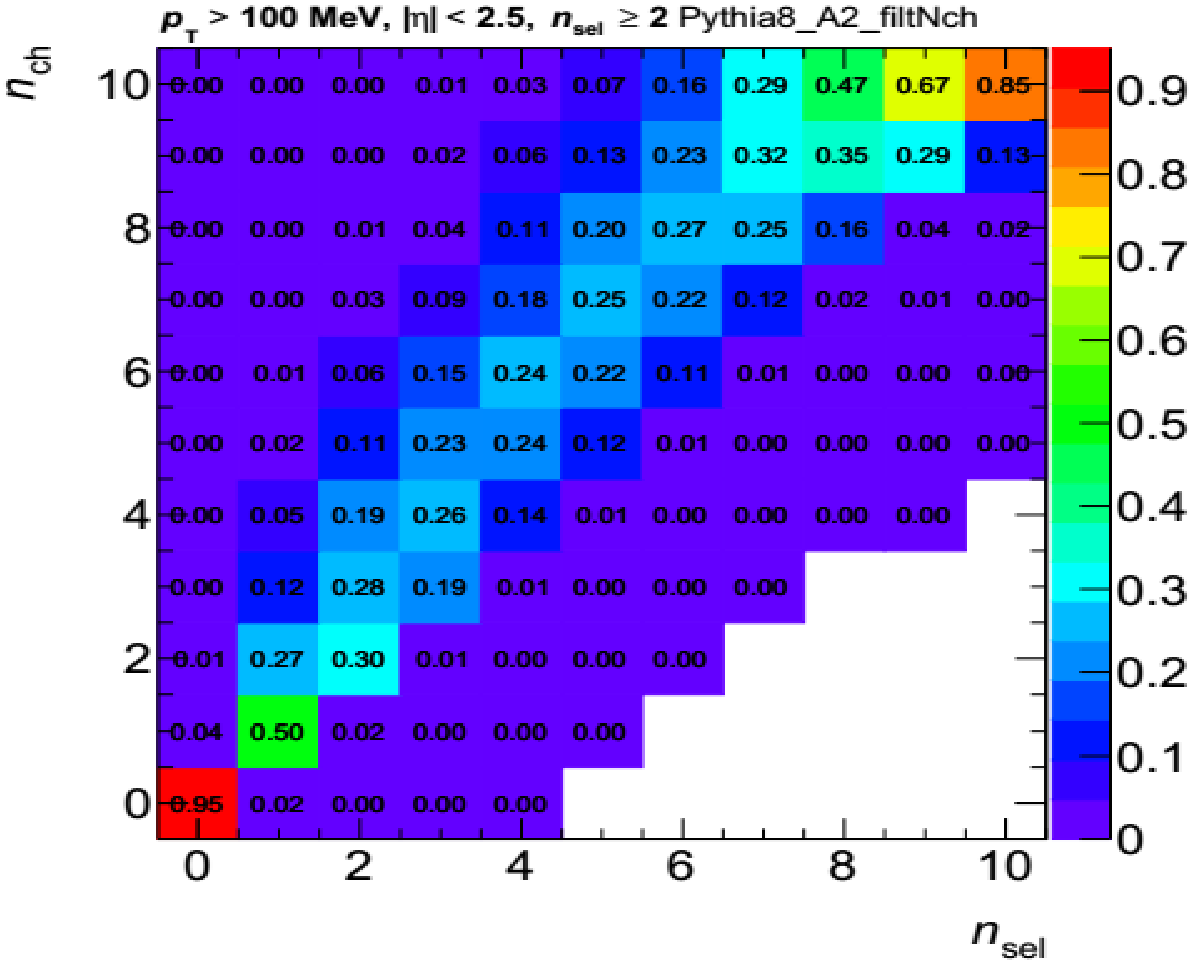

Migration matrix derived from Pythia 8 A2. Left: The full unfolding matrix. Right: The rows are normalized to one. The matrix is shown for the first iteration. There are several events with low n_{sel} but high n_{ch}. These events are caused by the tracking inefficiency where no track were found.

COULOMB CORRECTION

The measured N(Q) distribution for like or unlike signed particle (track) pairs in presence of the Coulomb interaction is given by:

$$N_{meas}(Q) = G(Q)N(Q)$$

where $N_{meas}(Q)$ is the measured distribution, *N(Q) is the distribution free of Coulomb correlations.*

Gamow penetration G(Q) factor $$G(Q) = \frac{2\pi\eta}{e^{2\pi\eta} - 1}$$

Sommerfeld parameter η $$\eta = \frac{\pm \alpha_m}{|Q|}$$

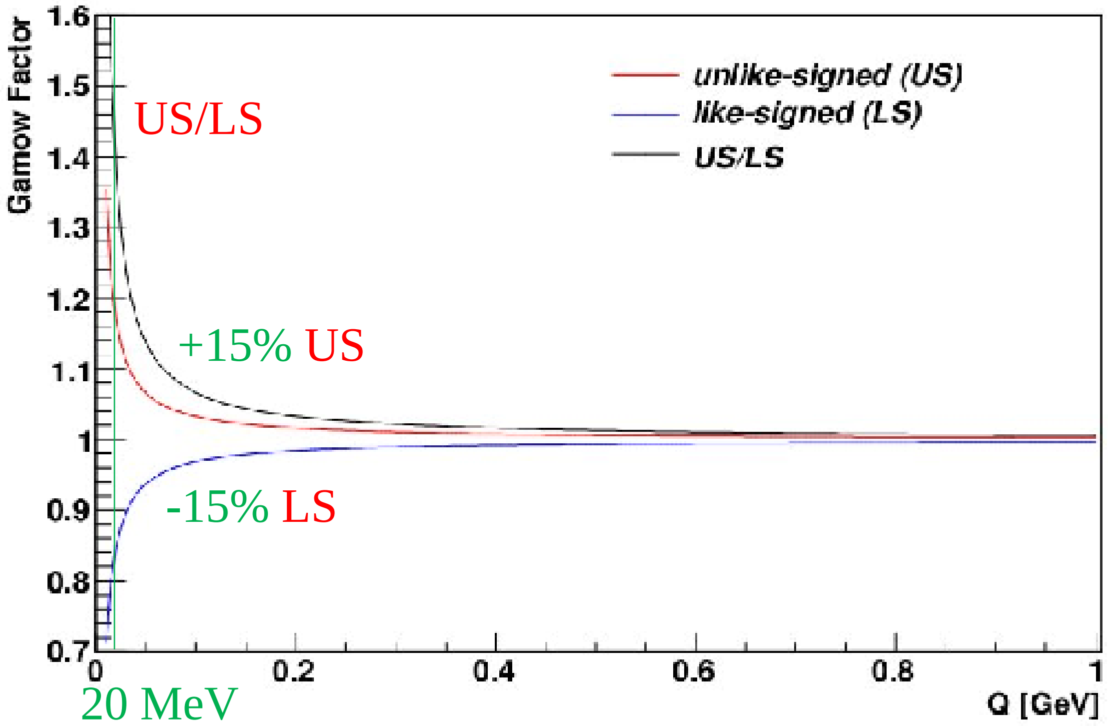

Gamow correction factor for like-signed (LS) particle pairs (blue), unlike-signed (US) particle pairs (red), for ratio of US to LS (black)

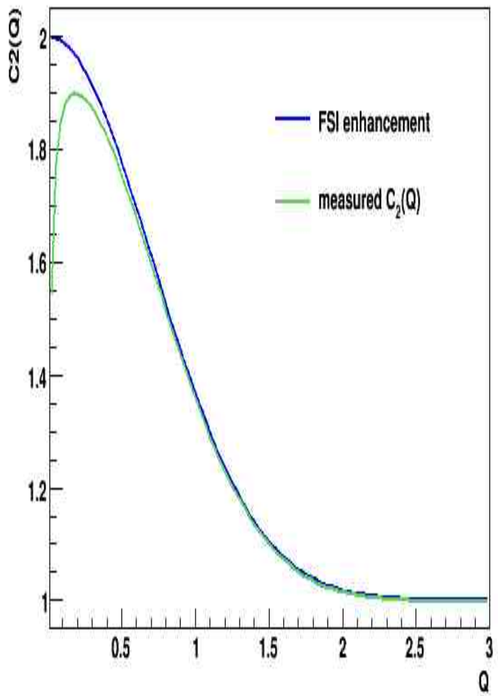

Ratio of the same two particle $C_2(Q)$ correlation functions with and without Coulomb correction. FSI is final state interactions

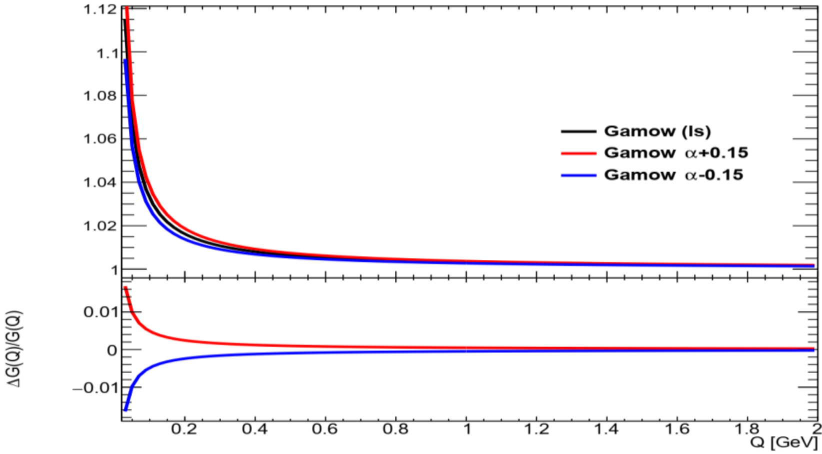

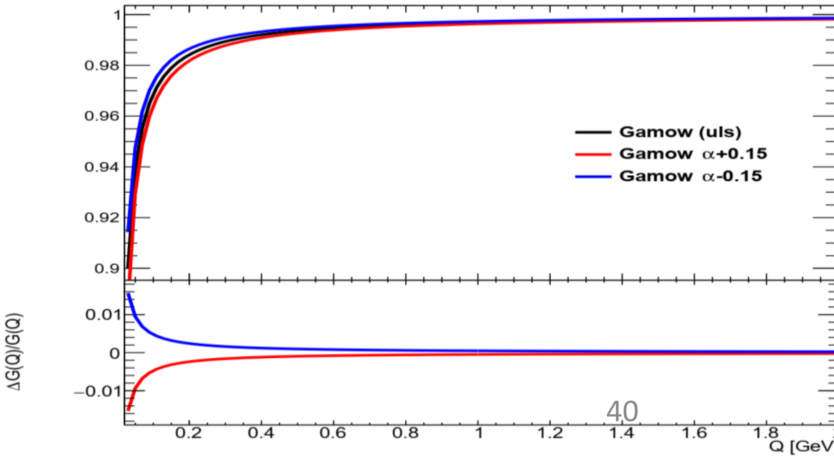

$R_2(Q)$ correlation function for OHP/UCP vs Transverse Thrust

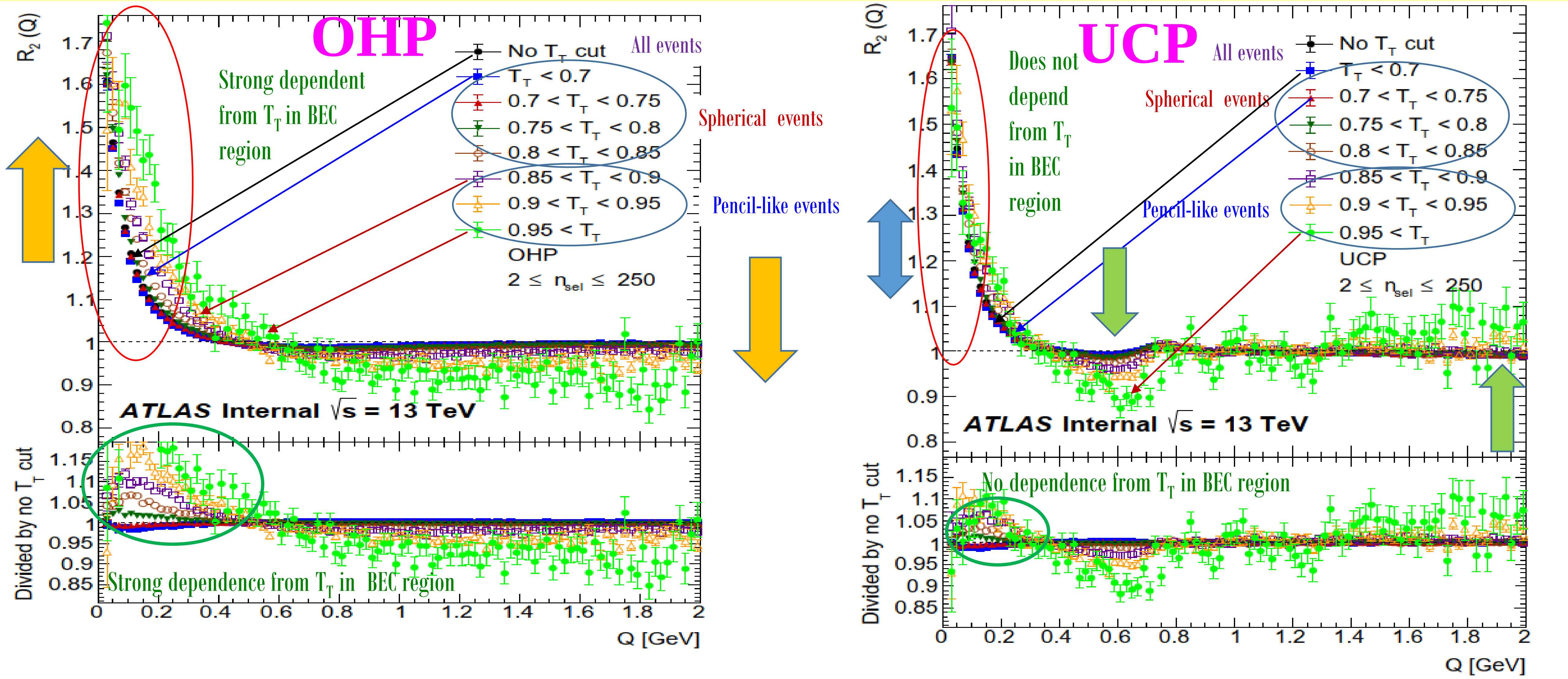

Multiplicity distributions for R_2(Q) correlation functions for the minimum-bias events with (left) OHP and (right) UCP reference samples versus Q for different thresholds of Transverse Trust

TRANSVERSE THRUST (T) & SPHEROCITY (S)

Transverse thrust is $T = \max_{\vec{n}_T} \frac{\sum |\vec{p}_T \cdot \vec{n}_T|}{\sum p_T}$, where the sum runs over all charged particles, the **thrust axis**, $\vec{n}_T$ maximizes the expression. For $n_{sel} \geq 2$. The solution for $\vec{n}_T$ is found iteratively: $\vec{n}_T^{(j+1)} = \frac{\sum \varepsilon(\vec{n}_T^{(j)} \cdot \vec{p}_T)\vec{p}_T}{|\sum \varepsilon(\vec{n}_T^{(j)} \cdot \vec{p}_T)\vec{p}_T|}$, where $\varepsilon(x>0)=1$ and $\varepsilon(x<0)=-1$.

Pencil-like event: two partons emitted in opposite directions in the transverse plane, with *T≈1 & S≈0*

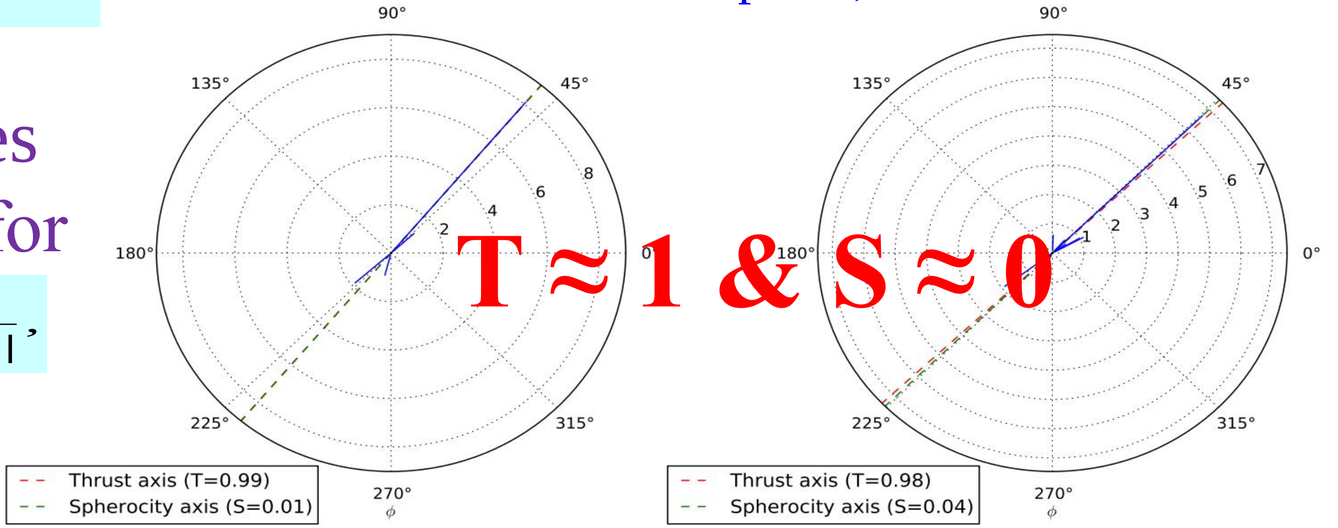

(a) Pencil-like events

Spherocity is $S = \frac{\pi^2}{4} \min_{\vec{n}=(n_x,n_y,0)^T} \left(\frac{\sum |\vec{p}_T \times \vec{n}|}{\sum p_T} \right)^2$, where the sum runs over all charged particles and the vector $\vec{n}_T$ minimizes the expression. For $n_{sel} \geq 2$.

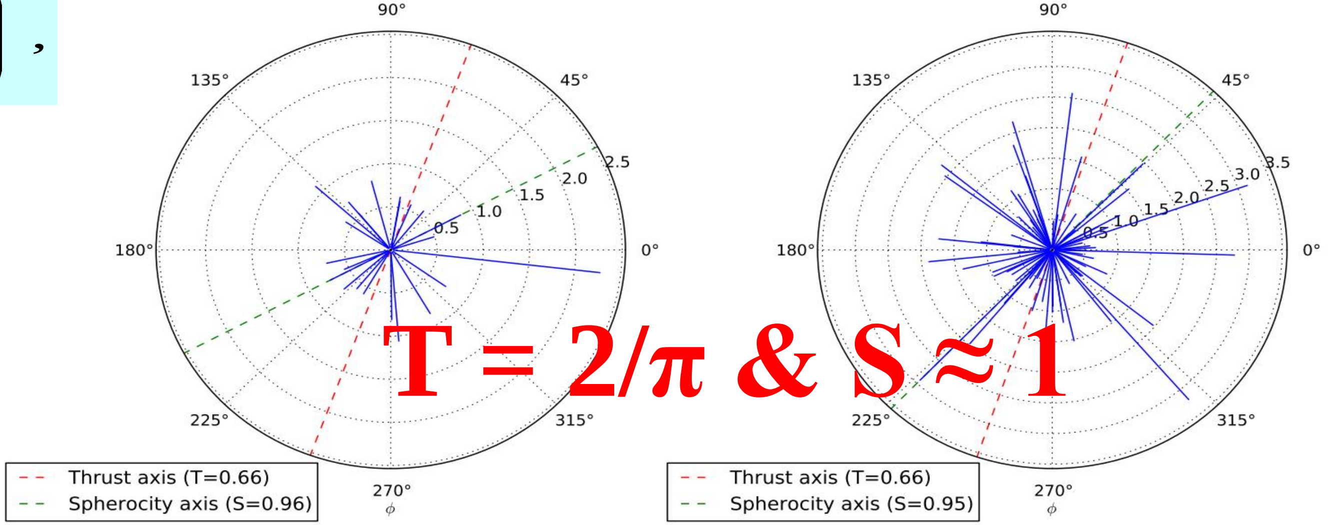

(b) Spherical events

Spherical event: containing several partons emitted isotropically, with T=2/π & S ≈ 1

COMPARISON OF $C_2(Q)$, $R_2(Q)$ WITH OHP REFERENCE SAMPLES AT 13 TEV

HMT events for multiplicity intervals

HMT events for k_T intervals

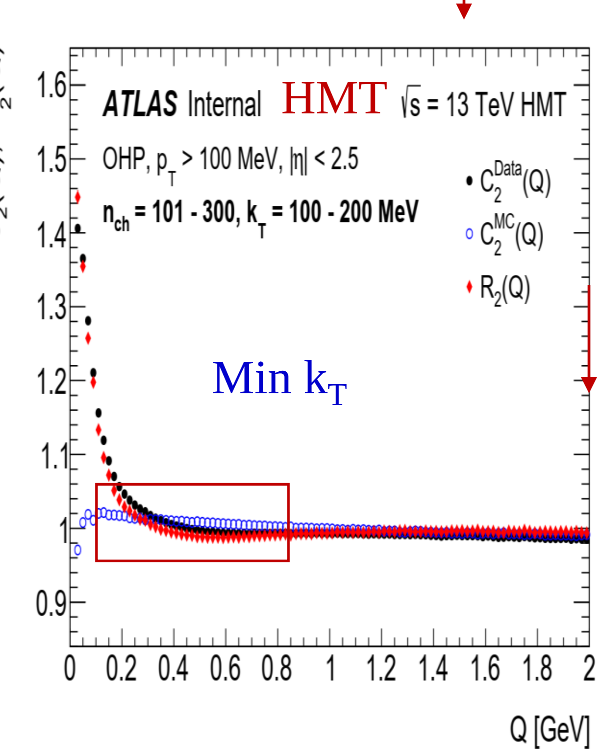

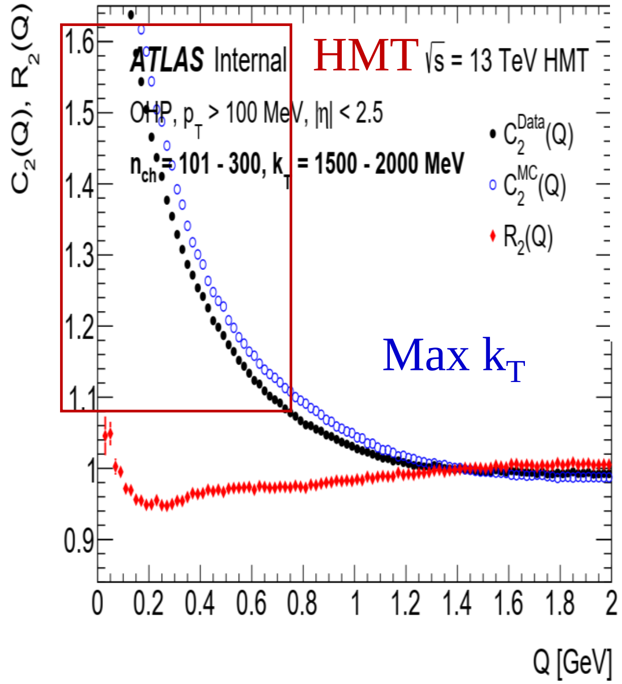

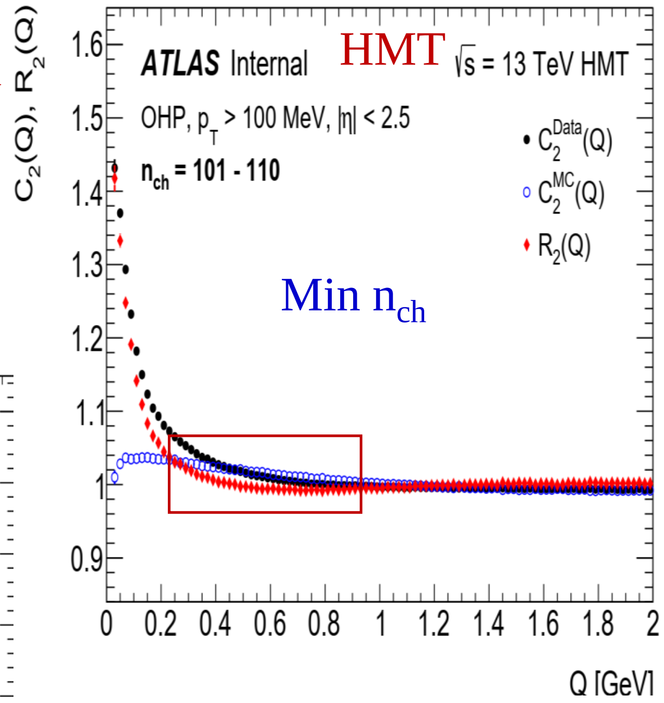

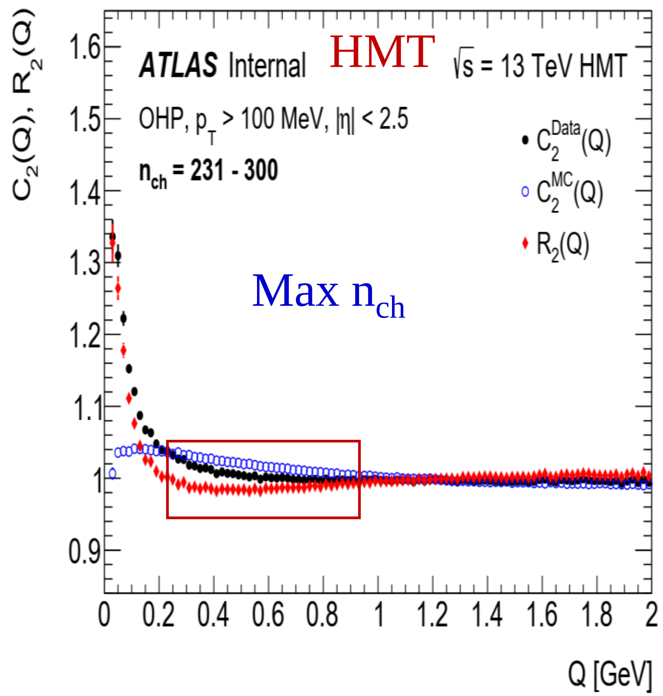

- Violation of the energy conservation low;
- Wide bump in the BEC region (Q<0.3 GeV) for $C_2^{MC}(Q)$;
- The bump size increases with k_T;
- $C_2^{MC}(Q)$ closer to $C_2^{data}(Q)$ for $k_T > 0.7$ GeV;
- Anticorrelation for $0.3<Q<1.0$ GeV ($C_2^{MC}(Q)>C_2^{data}(Q)$);
- The origin of bump: pencil-like events with jets.

Comparison of single-ratio two-particle correlation functions, $C_2^{data}(Q)$ and $C_2^{MC}(Q)$, with two-particle double-ratio correlation function, $R_2(Q)$, with the **OHP like-charge particles** pairs reference sample for HMT events.

$C_2(Q)$ correlation function for OHP/UCP vs Transverse Thrust

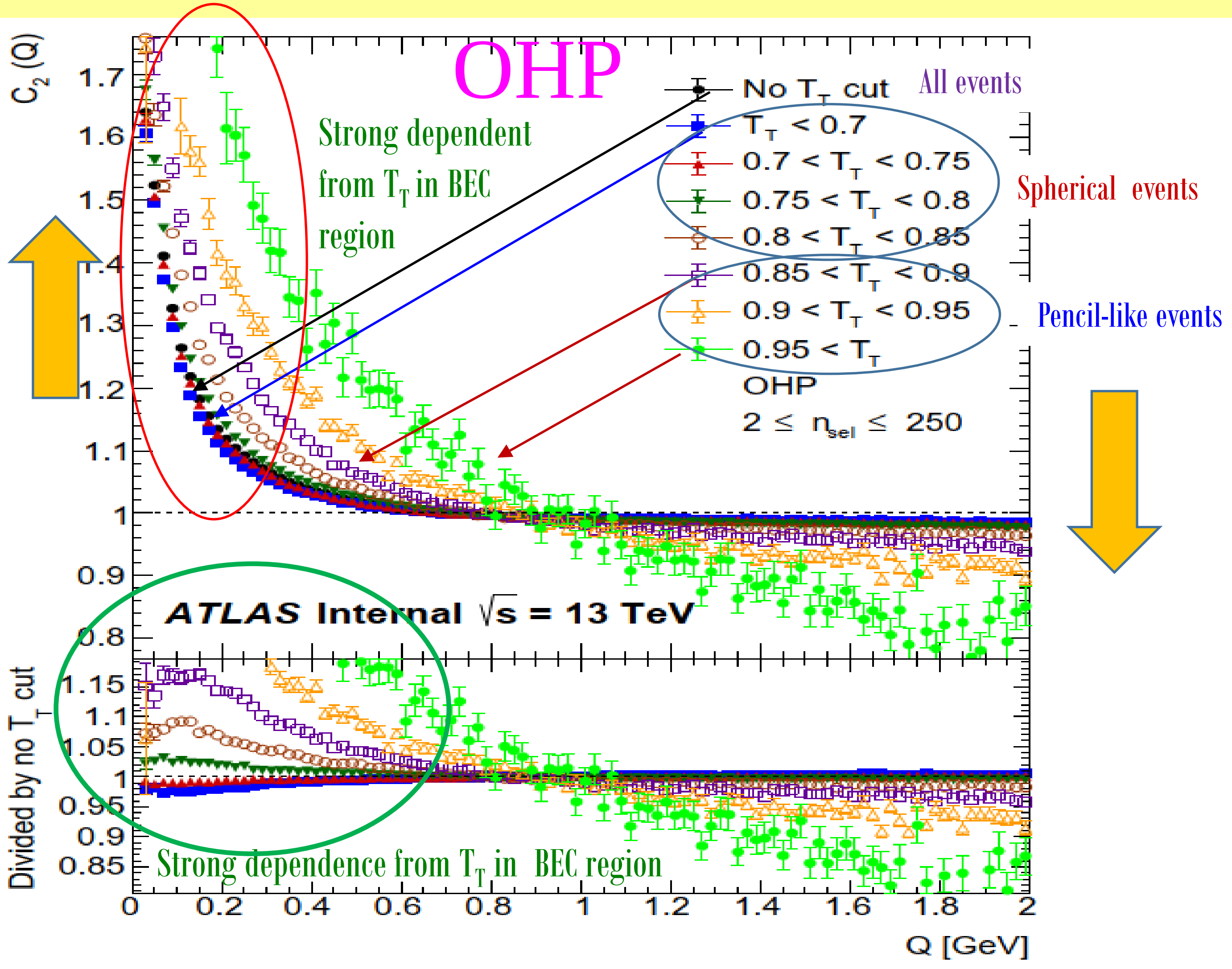

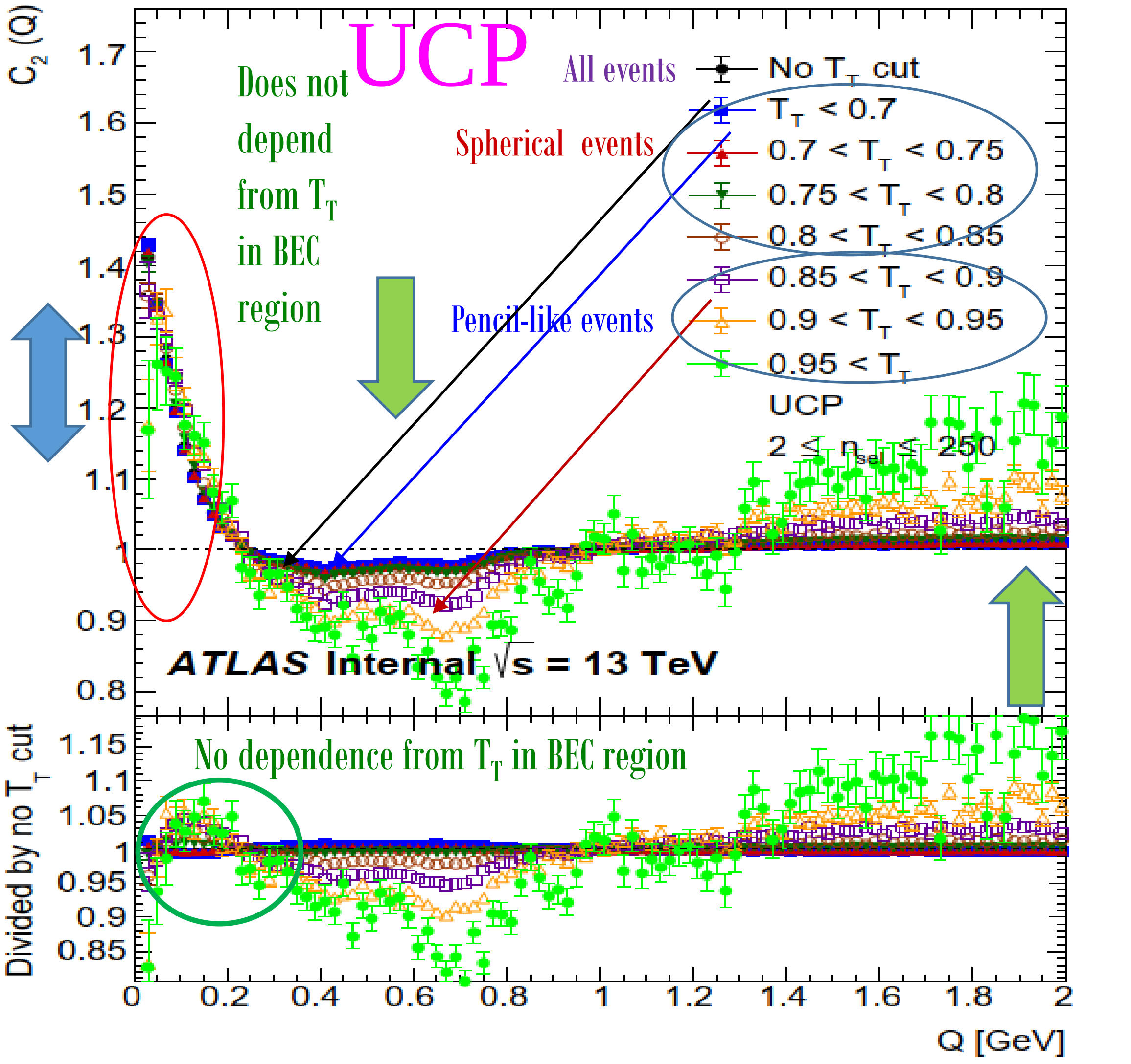

Multiplicity distributions for C_2 correlation functions for the minimum-bias events with (left) OHP and (right) UCP reference samples versus Q for different thresholds of Transverse Trust

CMS BEC13 results: p_T>200 MeV

CMS BEC@13 JHEP03 (2020) 014

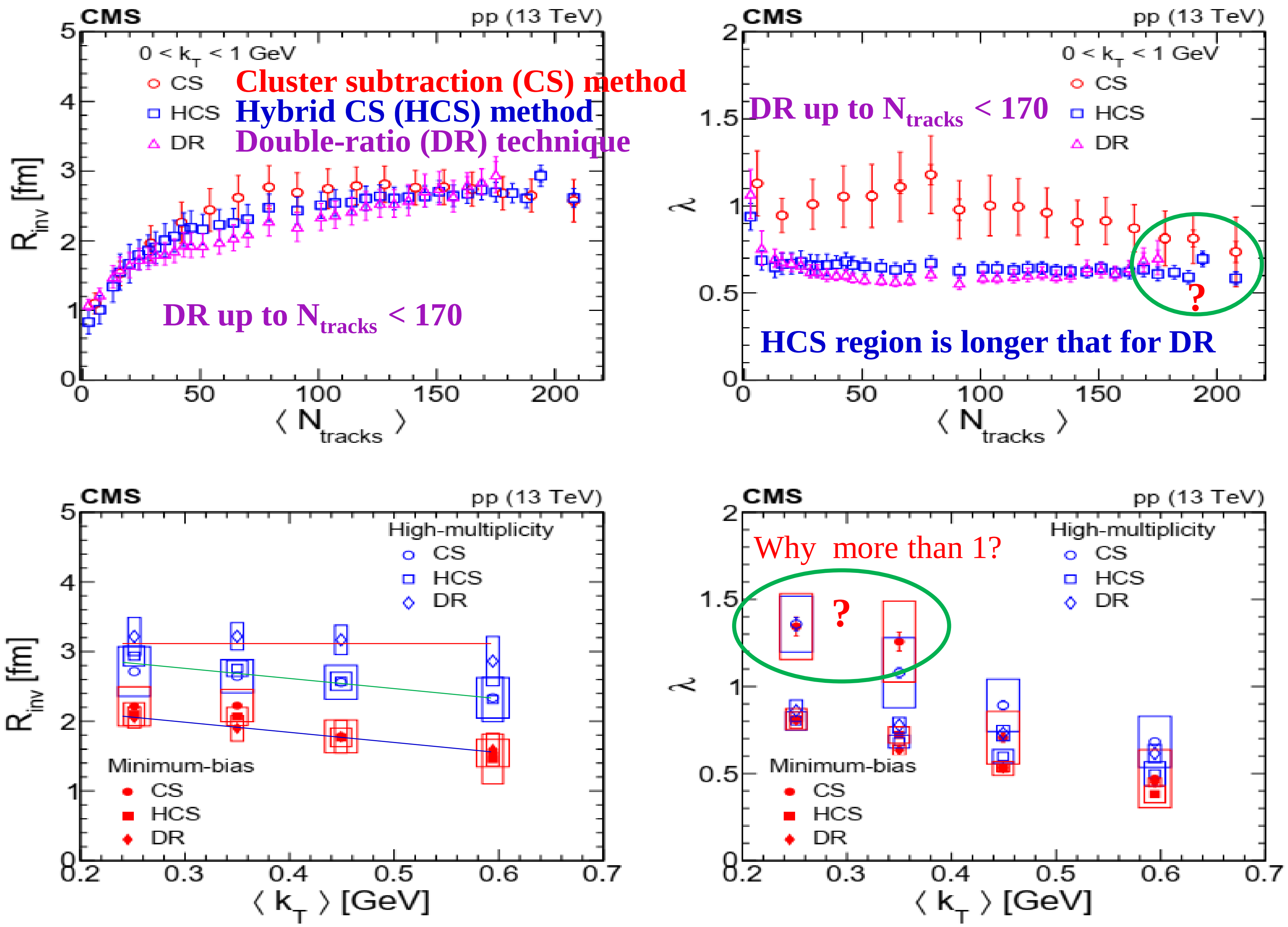

Results for $\boldsymbol{R_{inv}}$ and $\boldsymbol{\lambda}$ from the three methods as a function of multiplicity and k_T.

In the upper plots, statistical and systematic uncertainties are represented by internal and external error bars, respectively.

In the lower plots, statistical and systematic uncertainties are shown as error bars and open boxes, respectively

Comparison of BEC R & λ with UCP/OHP/MIX reference samples 0.9 & 7 TeV

ATL-COM-PHYS-2013-295, Support note for "Two-particle Bose-Einstein correlations in *pp* collisions at $\sqrt{s}$ = 900 GeV and 7 TeV measured with the ATLAS detector at the LHC"

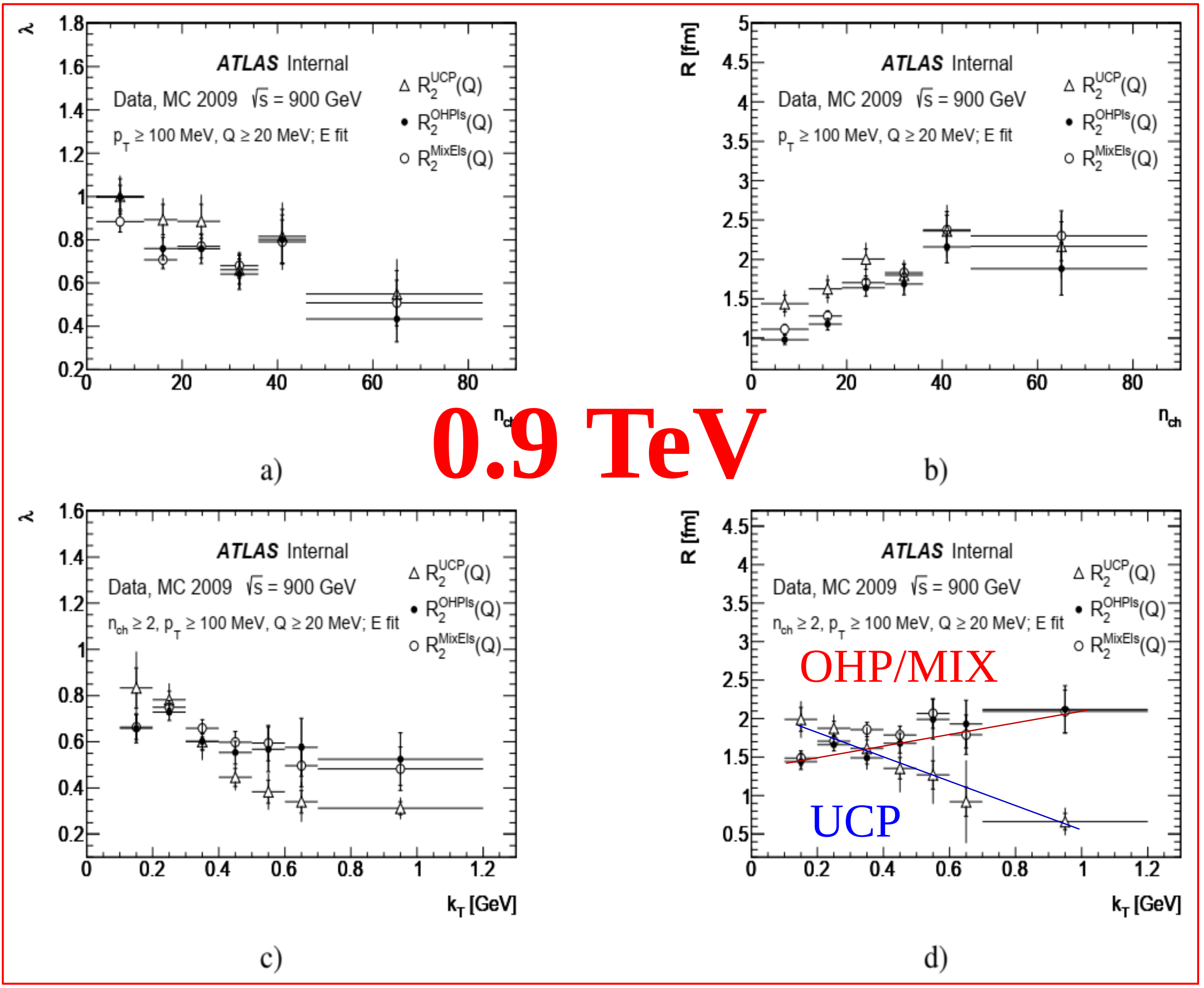

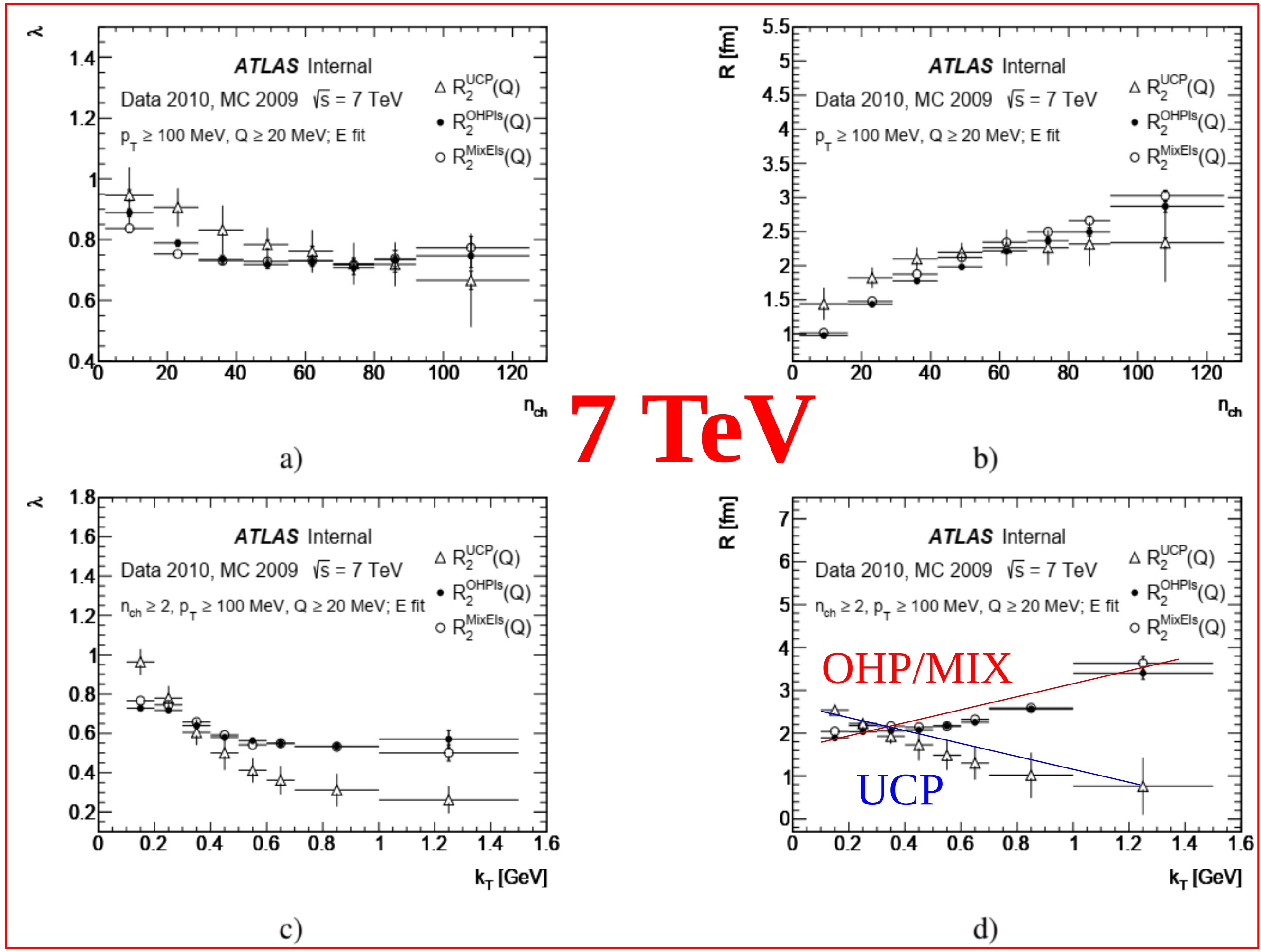

The comparison of the BEC parameters λ (left) and R (right) for the BEC results obtained from the fit the $R_2(Q)$ with the UCP, the OHP and MIX reference samples measured in pp collisions at 0.9 and 7 TeV for different multiplicity (top), k_T (bottom) intervals.

COMPARISONS: CMS BEC13 RESULTS

CMS BEC@13 JHEP03 (2020) 014

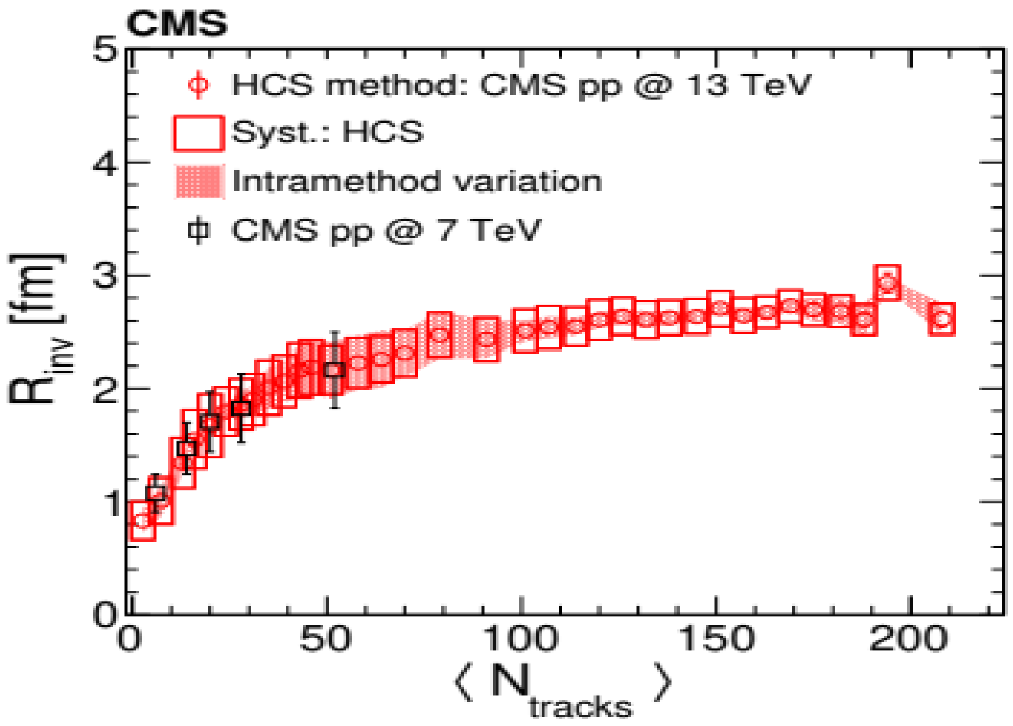

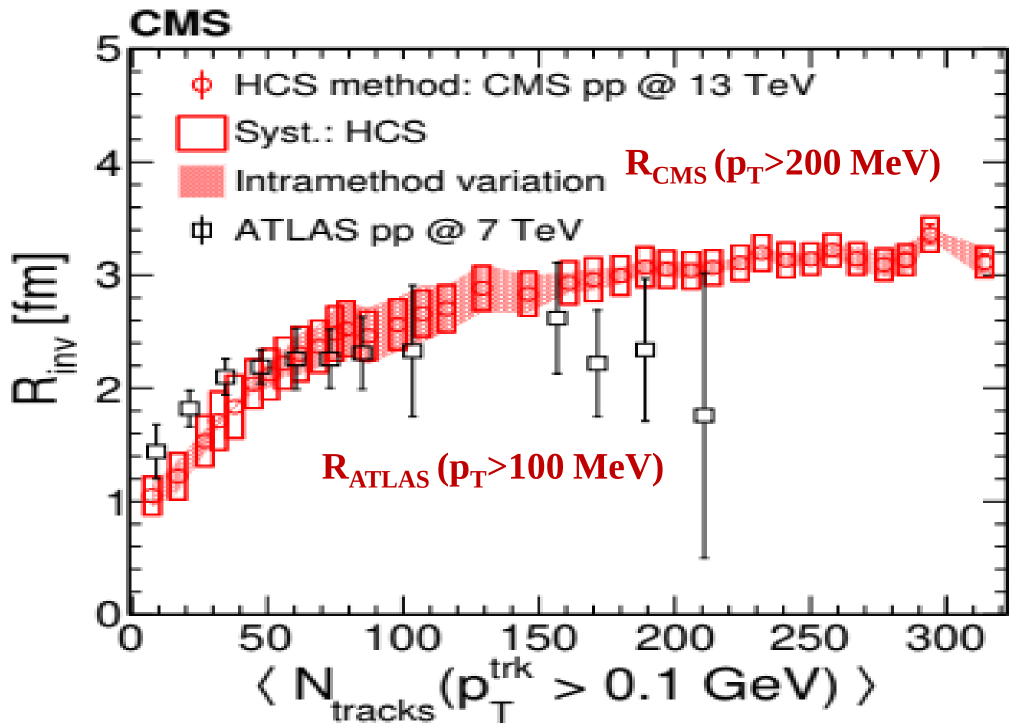

$K = N_{tracks}^{max}(p_T>100\ \text{MeV}) / N_{tracks}^{max}(p_T>200\ \text{MeV}) = 320/210 = 1.52$!!!

Figure 5. The R_{inv} fit parameters as a function of particle-level multiplicities using the HCS method in pp collisions at 13 TeV compared to results for pp collisions at 7 TeV from CMS (left) and ATLAS (right). Both the ordinate and abscissa for the CMS data in the right plot have been adjusted for compatibility with the ATLAS analysis procedure, as explained in the text. The error bars in the CMS [5] case represent systematic uncertainties (statistical uncertainties are smaller than the marker size) and in the ATLAS [15] case, statistical and systematic uncertainties added in quadrature.